

<https://helda.helsinki.fi>

Purification of Highly Active Alphavirus Replication Complexes Demonstrates Altered Fractionation of Multiple Cellular Membranes

Pietila, Maija K.

2018-04

Pietila , M K , van Hemert , M J & Ahola , T 2018 , ' Purification of Highly Active Alphavirus Replication Complexes Demonstrates Altered Fractionation of Multiple Cellular Membranes ' , Journal of Virology , vol. 92 , no. 8 , ARTN e01852-17 . <https://doi.org/10.1128/JVI.01852-17>

<http://hdl.handle.net/10138/298263>

<https://doi.org/10.1128/JVI.01852-17>

cc_by_nc_sa

acceptedVersion

Downloaded from Helda, University of Helsinki institutional repository.

This is an electronic reprint of the original article.

This reprint may differ from the original in pagination and typographic detail.

Please cite the original version.

Purification of highly active alphavirus replication complexes demonstrates altered fractionation of multiple cellular membranes

Running title: Activity of purified alphavirus replication complexes

Maija K. Pietilä^{1,*}, Martijn J. van Hemert², Tero Ahola^{1,*}

¹ Department of Microbiology, Faculty of Agriculture and Forestry, University of Helsinki, Viikinkaari 9 (PO Box 56), 00014 Helsinki, Finland

² Department of Medical Microbiology, Leiden University Medical Center (PO Box 9600), 2300 RC, Leiden, The Netherlands

* Correspondence

Abstract

Positive-strand RNA viruses replicate their genomes in membrane-associated structures; alphaviruses and many other groups induce membrane invaginations called spherules. Here, we established a protocol to purify these membranous replication complexes (RCs) from cells infected with Semliki Forest virus (SFV). We isolated SFV spherules located on the plasma membrane and further purified them using two consecutive density gradients. This revealed that SFV infection strongly modifies cellular membranes. We removed soluble proteins, the Golgi and most of the mitochondria, but plasma membrane, endoplasmic reticulum (ER) and late endosome markers enriched in the membrane fraction that contained viral RNA synthesizing activity, replicase proteins and minus- and plus-strand RNA. Electron microscopy revealed that the purified membranes displayed spherule-like structures with a narrow neck. This membrane enrichment was specific to viral replication as such a distribution of membrane markers was only observed after infection. Besides the plasma membrane, SFV infection remodeled the ER, and the co-fractionation of the RC-carrying plasma membrane and ER suggests that SFV may recruit ER proteins or membrane to the site of replication. The purified RCs were highly active in synthesizing both genomic and subgenomic RNA. Detergent solubilization destroyed the replication activity demonstrating that the membrane association of the complex is essential. Most of the newly made RNA was in double-stranded replicative molecules but the purified complexes also produced single-stranded RNA as well as released newly made RNA. This indicates that the purification established here maintained the functionality of RCs and thus enables further structural and functional studies of active RCs.

Importance

Similar to all positive-strand RNA viruses, the arthropod-borne alphaviruses induce membranous genome factories but little is known about the arrangement of viral replicase proteins and the presence of host proteins in these replication complexes. To improve our knowledge of alphavirus RNA-synthesizing complexes, we isolated and purified them from infected mammalian cells. Detection of viral RNA and *in vitro* replication assays revealed that these complexes are abundant and highly active when located on the plasma membrane. After multiple purification steps, they remain functional in synthesizing and releasing viral RNA. Besides the plasma membrane, markers

32 for the endoplasmic reticulum and late endosomes enriched with the replication complexes
33 demonstrating that alphavirus infection modified cellular membranes beyond inducing replication
34 spherules on the plasma membrane. We have here developed a gentle purification method to
35 obtain large quantities of highly active replication complexes, and similar methods can be applied
36 to other positive-strand RNA viruses.

37

38

39 **Keywords**

40 alphavirus, Semliki Forest virus, replication complex, purification, RNA replication, membrane
41 fractionation

42 **Introduction**

43 RNA viruses play a major role in emerging and re-emerging epidemics, and the most common RNA
44 viruses have a single-stranded genome of messenger-RNA polarity, i.e. positive-strand RNA (1, 2).
45 During replication, the genomic RNA serves as a template in the synthesis of a minus strand, which
46 then serves to produce more plus-strand RNAs (3). All eukaryotic positive-strand RNA viruses
47 replicate their genomes in membrane-associated complexes that concentrate replication
48 components, provide a structural framework and protect viral RNA from host defense mechanisms
49 (4-6). Depending on the virus, the replication membrane originates from the plasma membrane or
50 subcellular organelles such as mitochondria. Two main types of replication-associated membrane
51 modifications have been recognized (5). One type are double-membrane vesicles in which typically
52 multiple vesicles are interconnected via their outer membrane (7-10). The other type are vesicle-
53 like membrane invaginations called spherules, and the current view is that one or multiple double-
54 stranded RNA (dsRNA) intermediates, and thus the negative-strand RNA, reside within a spherule
55 and newly made, mature positive strands are released to the cytoplasm via a narrow neck that is
56 wide enough to allow the import of nucleotides and the export of positive-strand RNAs (11-16).

57 As a model system to study spherule invaginations we use an arthropod-borne alphavirus,
58 Semliki Forest virus (SFV). Alphaviruses are found on all continents and are known to cause
59 diseases ranging from mild febrile illnesses to encephalitis and prolonged arthritis (17). SFV is a
60 close relative of the re-emerged chikungunya virus (CHIKV) that causes arthralgia persisting in
61 some cases for years (18, 19). The alphavirus genome encodes two polyproteins. The
62 nonstructural polyprotein P1234 is first cleaved to P123 and nonstructural protein 4 (nsP4), which
63 form an early replication complex (RC) that synthesizes minus-strand RNA using the genome as a
64 template (20, 21). Further cleavage of P123 then yields a late RC consisting of nsP1 to nsP4 and
65 making plus strands from the minus-strand RNA (20). nsP4 is the core RNA-dependent RNA
66 polymerase (RdRp) but RNA synthesis requires also nsP1, which is the capping enzyme and
67 membrane anchor of RCs, nsP2, which is the protease and helicase, and nsP3, which interacts with
68 multiple host proteins (20, 22-31). The second polyprotein, which is translated from a subgenomic
69 RNA, is cleaved to the capsid and envelope proteins (3).

70 The role of spherules in alphavirus replication was suggested in the 1960s and 1970s when it
71 was observed that viral RNA synthesis co-localizes with spherule-carrying cytopathic vacuoles
72 (CPVs) in infected cells and the RNA-synthesizing activity, viral RNA and CPVs were found to be
73 enriched in the same fraction after isolation (32-34). Spherules (diameter of ~50 nm) contain

74 electron dense material and can be immunostained for dsRNA, indicating that the replicative
75 dsRNAs are located inside the spherules (35, 36). Furthermore, nsPs co-localize with CPVs and with
76 dsRNA staining (15, 35, 37), and it has been shown that the template RNA length determines
77 spherule size strengthening the view of spherules as replication sites (13). Although CPVs revealed
78 the role of spherules in viral RNA replication, spherules are first formed at the plasma membrane.
79 In SFV-infected cells, spherules are then internalized and after fusion with late endosomes they
80 accumulate in perinuclear area in CPVs (15). In contrast, Sindbis virus (SINV) and CHIKV spherules
81 predominantly stay on the plasma membrane (35, 38).

82 Functional *in vitro* studies on alphavirus replication have to a large extent focused on crude
83 membrane preparations showing that most of the minus-strand RNA as well as RNA-synthesizing
84 activity are found in a membrane pellet prepared from infected cells (11, 39). Alphaviruses
85 synthesize in cells and *in vitro* the same RNA species, genomic and subgenomic single-stranded
86 RNA (ssRNA) as well as double-stranded replicative forms (RFs) and replicative intermediates (RIs)
87 (11, 40, 41). In addition, RNA II corresponding to the 5' end of the genome up to the subgenomic
88 promoter is made but its function remains unclear (11, 39, 42). However, only RNA of positive
89 polarity is synthesized *in vitro* (11, 39). Cytosolic host factors are not required in alphavirus RNA
90 synthesis *in vitro* in contrast to positive-strand RNA nidoviruses (11, 39, 43-45). In order to study
91 both the structure and the molecular mechanisms of these membranous RCs, purified and active
92 complexes must be obtained. Alphavirus RCs have been purified in sucrose- and glycerol-density
93 gradients indicating that these complexes are indeed membrane associated (32, 40, 41, 45-47).
94 However, purification, which may include detergent solubilization, often yields poor replication
95 activity and only two to three virus-specific proteins have been observed in these complexes.
96 Thus, we still lack an approach to obtain purified, fully functional complexes amenable for
97 structural studies such as cryo-electron microscopy, and there is no structure available for the
98 alphavirus RCs or RdRp.

99 Here we report a purification method for SFV RCs, and our aim was to maintain the
100 functionality, integrity and morphology of the RCs that enables us to study their biological
101 mechanisms. First, we show that RCs isolated from SFV-infected cells are stable and then further
102 purify these. We demonstrate that the purified RCs are highly active in RNA synthesis and release
103 newly synthesized RNA strands. We also show that SFV infection causes extensive modification of
104 cellular membranes by inducing spherules on the plasma membrane, but the effects reach
105 multiple intracellular membranes.

Results

Isolated SFV RCs are stable

A number of parameters were tested to study if SFV RCs preserve their replication activity under different conditions and are thus amenable for purification. Metabolic labeling has shown that SFV RCs are most active in RNA synthesis in baby hamster kidney (BHK) cells at 4-5 h p.i. at a MOI of 50 (39). Thus, post-nuclear supernatant (PNS) was prepared from SFV-infected cells (MOI of 50) at 4 h p.i. and *in vitro* RNA synthesis was analysed by measuring the incorporation of ³²P-CTP into viral RNA (Fig. 1). Incorporation was readily detected after a 5-min reaction time, and the signal rapidly increased up to 60 min (Fig. 1A and B). Consequently, 1-h reaction time was routinely used unless otherwise stated. Furthermore, SFV PNS could be diluted at least 100-fold without the loss of replication activity (Fig. 1C).

The highly active and robust RNA synthesizing activity *in vitro*, which tolerated dilution, indicated that SFV RCs are suitable for purification. Next we tested if RCs remain active during the prolonged incubation times that are required to perform the purification procedures. The complexes remained active throughout a 48-h incubation at 4°C (Fig. 1D). In-gel hybridization revealed that the endogenous minus-strand RNA was also stable while most of the endogenous plus-strand RNA was digested already after 3 h (Fig. 1E). This confirms the idea that in cells most plus strands are released to the cytosol, and thus in PNS they are susceptible to cellular RNases, and the minus-strand RNA resides inside the spherules as part of double-stranded RNA molecules in a form that protects them from nucleases. We also determined the stability of RCs in the density gradient medium iodixanol, which is used for subcellular fractionation, and after a 24-h incubation, RCs were still highly active and minus-strand RNA was stable (Fig. 1D and E). Bovine serum albumin (BSA; 1 mg/ml) was observed to boost *in vitro* replication, on average about 120% (Fig. 1D). Thus, in further experiments BSA was routinely used in the reaction mixture. SFV RNA synthesis *in vitro* could be inhibited by the chain terminator 3'-dCTP (Fig. 1D).

Then, we determined the tolerance of detergents using PNS and the *in vitro* replication system. *In vitro* replication activity of SFV RCs was sensitive to all detergents tested but more sensitive to anionic sodium deoxycholate (DOC) and sodium dodecyl sulfate (SDS) than to non-ionic n-Octylglucoside and Triton X-100 (Tx-100) (Fig. 1F). 1% DOC and SDS caused the loss of both the minus-strand template and replication activity indicating that spherules were destroyed and the minus-strand RNA was exposed to cellular nucleases (Fig. 1F). In contrast, about 80% and 90%

138 of the minus-strand RNA present in the untreated sample was recovered after 1% n-Octylglucoside
139 and Tx-100 treatments, respectively. Thus, here the partial loss of the activity could be due to
140 disruption of protein-membrane interactions.

141 Finally, we tested which subcellular location of spherules is the most suitable for purification
142 by utilizing drug treatments. It has been reported that wortmannin blocks SFV spherules mainly on
143 the plasma membrane, while nocodazole treatment leads to their accumulation in small endocytic
144 vesicles (15). In the absence of drugs, spherules accumulate in CPVs. PNS was prepared from
145 untreated and drug-treated cells infected at a MOI of 500 and collected at 4 h p.i. Quantification of
146 in-gel hybridizations showed that PNS from wortmannin-treated cells contained the highest
147 amount of endogenous minus- and plus-strand RNA indicating that also the number of RCs was
148 the highest (Fig. 2A and B). Importantly, RCs were highly active in RNA synthesis *in vitro*
149 independent of their subcellular location, although wortmannin-treated samples gave the highest
150 activity (Fig. 2C). The observed *in vitro* RNA synthesis was consistent with that obtained in cells
151 using metabolic labeling (15). The wortmannin treatment and a MOI of 500 resulted in about the
152 same amount of the minus-strand RNA as a MOI of 50 without drug treatment (Fig. 2B). However,
153 the amount of the plus-strand RNA was doubled (Fig. 2A). This phenomenon was also observed
154 with nocodazole-treated and untreated cells infected at a MOI of 500 when compared to
155 untreated cells infected at a MOI of 50 (Fig. 2A and B). If we assume that the minus-strand RNA
156 represents spherules, this indicates that at the higher MOI, RCs are formed faster and have more
157 time to synthesize plus strands.

158 159 **SFV RCs distribute in both the supernatant and the mitochondrial pellet**

160 Due to the high abundance and activity, we chose to purify plasma membrane-derived spherules
161 and the optimized purification method is summarized in Fig. 3. SFV-infected cells (MOI 500) were
162 treated with wortmannin at 1.5 h p.i. and harvested in an isotonic homogenization buffer at 4 h
163 p.i. Dounce homogenization was used to lyse cells in the previous assays, but it caused disruption
164 of mitochondria and thus cells were lysed for RC purification by passaging through a 22-G needle.
165 Nuclei and any remaining intact cells were removed by differential centrifugation yielding PNS.
166 Further centrifugation to remove mitochondria at $7,000 \times g$ yielded a P7 pellet and S7
167 supernatant. The same amount of cells were seeded for mock and virus infection but when cells
168 were collected, mock samples contained twice the amount of cells compared to the infected
169 samples. However, both cell lysates contained similar amounts of proteins (~13 mg/ml) indicating

170 that there were more proteins in infected cells than in mock cells. PNS (~3.2 mg/ml) and S7 (~2.6
171 mg/ml) prepared from SFV-infected cells contained more protein than the corresponding samples
172 from mock cells (~2.0 mg/ml in PNS and ~1.7 mg/ml in S7) indicating that infected cells lysed
173 better than mock cells.

174 Most of the proteins and about half of the lipids present in mock and SFV PNS distributed to
175 S7 (Fig. 4A and B). In order to detect lipids, we utilized an approach to stain lipoproteins with
176 Sudan Black B after polyacrylamide gel electrophoresis (see Materials and Methods). However,
177 gels were stained after a short electrophoresis to allow detection of species below a 10-kDa
178 marker. Distribution of different viral and cellular markers was further studied by Western blotting
179 (Fig. 4C). Most of nsP2, nsP3 and nsP4 as well as about 50% of nsP1 were found in the viral S7. SFV
180 capsid protein was also mainly found in the S7 fraction. The Golgi matrix protein of 130 kDa
181 (GM130), the endoplasmic reticulum (ER) marker calnexin, the mitochondrial marker succinate
182 dehydrogenase subunit A (SDHA), and the cytosolic marker β -actin showed a similar distribution
183 into S7 and P7 fractions in both mock and virus samples. GM130 was exclusively detected in S7
184 and β -actin was more prominent in S7 than in P7. Most of SDHA distributed in the P7 pellet, and
185 about half of calnexin was found in S7. About half of the plasma membrane calcium pump ATPase
186 (PMCA) was found in the mock S7 while in the virus-infected samples it was more prominent in S7
187 than in P7. In both mock and virus-infected samples the late endosomal marker Rab7 was more
188 prominent in S7 than in P7 but the enrichment was stronger in the mock samples.

189 *In vitro* replication activity present in the viral PNS, S7 and P7 fractions was analysed by
190 quantifying the incorporation of 32 P-CTP into SFV 42S RNA (Fig. 4D). About 50% and 30% of the
191 PNS activity was recovered in S7 and P7, respectively. In-gel hybridization showed that the minus-
192 strand RNA distributed equally to S7 and P7 (Fig. 4E) indicating that differential centrifugation
193 caused a partial loss of replication activity in the pellet fraction. Approximately 60% of the
194 genomic RNA was found in S7.

195

196 **SFV infection modifies the properties of cellular membranes**

197 We selected the S7 fraction for further purification in density gradients (Fig. 5 and 6) as more than
198 half of the active RCs remained in this fraction. RCs were first purified from the S7 fractions by
199 sedimentation in a 10-20% iodixanol-step gradient (Fig. 3) by loading 500 μ l of S7 on the top of a
200 12-ml density gradient, resulting in ~0.9 and 1.3 mg of proteins loaded from mock and virus-
201 infected samples, respectively. Signals from the cellular markers were comparable in the S7

202 fractions from mock and SFV-infected cells (Fig. 5 and 6). After sedimentation, a light-scattering
203 band was detected in every interphase as well as close to the gradient surface. Gradients were
204 fractionated, and the protein pattern in each fraction was determined by SDS-PAGE (Fig. 5A). Most
205 proteins stayed in the top fractions of sedimentation gradients derived from the S7 fraction of
206 mock (labeled mock) or SFV-infected (labeled SFV) cells, although the latter resulted in the
207 detection of more proteins especially in fr. 5. Lipids were detected in all fractions that correspond
208 to the bands and in the pellet (Fig. 5B). In both gradients, lipids concentrated in fr. 5 and 6 (band
209 3). However, fr. 3 and 4 (band 2) of the mock gradient contained more lipids than the
210 corresponding fractions of the SFV gradient.

211 Western blotting revealed the distribution of viral and cellular markers between gradient
212 fractions (Fig. 5C). In the SFV gradient, nsPs concentrated in fr. 1, 3-4 and 5-6 corresponding to
213 bands 1, 2 and 3, respectively. SFV capsid protein was observed in fr. 1-8. The Golgi marker stayed
214 on the top of both gradients, and the remaining mitochondrial marker was mainly on the top and
215 a minor amount was detected in fr. 5. In the mock gradient, the plasma membrane marker PMCA
216 mostly stayed on the top while in the SFV gradient it concentrated in fr. 1 and 5-6 (band 3). To
217 further study the distribution of the plasma membrane, another plasma membrane marker, Na,K
218 ATPase, was included, and this marker gave similar distribution in the sedimentation gradients as
219 PMCA although PMCA showed stronger concentration in fr. 5-6 (band 3) in the SFV gradient. The
220 late endosomal marker Rab7 predominantly stayed on the top of the mock gradient while in SFV it
221 concentrated in both fr. 1 and 5-6 (band 3). Lysosome-associated membrane protein 2 (LAMP-2),
222 which is a marker for the late endosomes and lysosomes, showed a different distribution
223 compared to Rab7. In the mock gradient LAMP-2 concentrated in fr. 2-5 and in the SFV gradient in
224 fr. 1-5. The ER marker calnexin concentrated in the mock gradient in fr. 3-4 (band 2) and fr. 5-6
225 (band 3) and in the SFV gradient in fr. 5-6 (band 3). To further examine ER distribution, two
226 additional markers for ER were included. CLIMP-63 (cytoskeleton-linking membrane protein 63),
227 also known as CKAP-4 (cytoskeleton-associated protein 4), is predominantly found in ER sheets
228 (48) and reticulon 4B (RTN4B), also known as Neurite outgrowth inhibitor B (Nogo-B), localizes to
229 ER tubules and sheet edges (49). CLIMP-63 showed a similar distribution as calnexin although an
230 additional band was detected in fr. 1. RTN4B was found in fr. 1-5 of the mock gradient while in the
231 SFV gradient RTN4B concentrated in fr. 5-6 (band 3) similar to calnexin and CLIMP-63. The
232 cytosolic marker β -actin concentrated in the top fractions but in the SFV gradient it was also found
233 in fr. 5-6 (band 3). We also tested addition of 150 mM KCl to the cell lysate if higher salt

234 concentration was required to keep membranes from aggregating but no effect in sedimentation
235 was observed indicating that the results were not due to unspecific membrane aggregation.

236 An *in vitro* replication assay showed that most of SFV replication activity was in fr. 5-6 (band
237 3) of the sedimentation gradient (Fig. 7B) and thus this band at density of 1.10-1.11 g/ml was
238 collected for further purification. The final step in the purification was equilibrium centrifugation
239 in a 10-30% iodixanol-step gradient as shown in Fig. 3. After flotation, two light-scattering bands
240 were observed and gradients were fractionated. Fr. 10-12 represent 30% iodixanol containing the
241 band 3 collected from the sedimentation gradient. The upper band in the flotation gradient (band
242 1 in Fig. 3) was considerably weaker than the other band (band 2 in Fig. 3) and detectable proteins
243 and lipids concentrated in the area of the band 2 or lower fractions. Coomassie staining revealed
244 very little protein in the mock fractions (Fig. 6A). In the SFV gradient, proteins were mainly
245 observed in fr. 4 (band 2) as well as in fr. 9-12. Lipids were detected in both gradients in fr. 4 albeit
246 SFV gave a much stronger signal (Fig. 6B). In the mock gradient, Western blotting detected only a
247 weak calnexin signal in fr. 3 and 4 (Fig. 6C). In the SFV gradient, nsPs and capsid protein
248 concentrated in fr. 4, except for that nsP2 and capsid were also detected in fr. 9-12 indicating that
249 nsP2 and capsid protein in these fractions did not float and thus were not membrane associated.
250 The plasma membrane marker PMCA, late endosome marker Rab7 and ER marker calnexin also
251 concentrated in fr. 4. In addition, β -actin and the residual mitochondria were detected in fr. 4.
252 Golgi was hardly detectable. The density in fr. 4 was 1.11 g/ml. As viral nsPs and PMCA, Rab7 and
253 calnexin concentrated in fr. 4 in the SFV gradient, fr. 3-5 were further studied using additional
254 cellular markers (Fig. 6D). The plasma membrane marker Na,K ATPase as well as ER markers
255 CLIMP-63 and RTN4B also concentrated in fr. 4 in the SFV gradient while these markers were
256 undetectable in the mock fr. 3-5. Interestingly, LAMP-2, a marker for the late endosomes and
257 lysosomes, was undetectable in fr. 3-5 of both mock and SFV gradient.

258 We next assayed where SFV minus- and plus-strand RNA as well as 18S ribosomal RNA
259 (rRNA) distributed in the sedimentation and flotation gradients (Fig. 7A). 18S rRNA concentrated in
260 sedimentation fr. 4, and only a small amount was detected after flotation, in fr. 9-12 indicating
261 that the detected rRNA did not float. After sedimentation, the minus- and plus-strand RNA were
262 mainly recovered in fr. 1, 3-4 and 5-6, and after flotation, both concentrated in fr. 4.
263 Approximately 20% of the minus-strand RNA present in S7 was recovered in flotation fr. 4.

264 In both sedimentation and flotation gradients 32 P-CTP incorporation co-localized with the
265 endogenous minus-strand RNA (Fig. 7), and high *in vitro* replication activity was observed after the

266 purification. The RCs in the flotation fr. 4 (band 2) were designated as purified RCs and collected
267 for further characterization. The average protein concentration of the purified RCs from three
268 purifications was 0.02 mg/ml indicating that less than 1% of the proteins present in S7 were
269 remaining. However, the recovery of the activity present in S7 was approximately 20% when the
270 ³²P-CTP incorporation into the genomic RNA was compared (Fig. 7C). The purified RCs synthesized
271 both genomic and subgenomic RNA but RNA II was observed only in sedimentation fr. 1 and 3 (Fig.
272 7B and C).

273

274 **Purified RCs display spherule-like structures and release newly made RNA**

275 Electron microscopy of the purified RCs and the corresponding membrane fraction from mock cells
276 revealed sheets, vesicles and some tubule-like membranes (Fig. 8). Sheets, which might be derived
277 from the plasma membrane or ER, were observed in both samples (Fig. 8A). Sheets or vesicles with
278 multiple, spherical invaginated membranes were typical of the purified RCs and could not be
279 detected in the mock samples (Fig. 8B-I). The diameter of these invaginations was similar to that of
280 spherules, about 50 nm, and some of them showed a dark spot in the middle, most likely
281 representing RNA. In addition, membrane sheets displaying smaller round structures, which may
282 represent narrow spherule necks, were observed (Fig. 8C). A few nucleocapsids were also found
283 close to the spherule-like structures (Fig. 8D).

284 To determine the stability of the newly made RNA, *in vitro* replication reactions were
285 terminated by adding the nucleoside analogue 3'-dCTP followed by a chase for 3 h (Fig. 9A). In the
286 unternminated control samples, the amount of the ³²P-CTP-labeled genomic RNA increased
287 approximately 1.7-fold or 2.5-fold in the reactions containing the S7 or purified RCs, respectively.
288 After termination, the level of the labeled genomic RNA slowly decreased in both S7 and purified
289 RCs, with a similar rate. However, the half-life was more than 180 min. In contrast, when a capped
290 *in vitro* transcript of Tmed RNA, which contains the SFV 5' and 3' untranslated regions as well as
291 the subgenomic promoter, was added in the reactions, it was rapidly degraded in the S7 sample
292 and the half-life was less than 15 min. This indicated that the newly synthesized SFV RNA was
293 protected in the S7 sample and for CHIKV, it has been proposed that membrane or polysome
294 association, RNA structure or encapsidation protects newly made ssRNA from cellular nucleases
295 (11). In the reaction mixture containing purified RCs, the Tmed RNA was approximately as stable
296 as the viral replication products suggesting that purification removed most of the cellular
297 nucleases.

298 As added RNA remained relatively stable in the purified preparations, we tested if the
299 purified RCs are able to utilize an exogenous template RNA. However, no additional RNA products
300 were synthesized when the Tmed template was provided in addition to the endogenous one (Fig.
301 9B) indicating that once a functional RC has been formed it is unable to replicate another
302 template. We also tested if RCs remained sensitive to detergents now when cellular nucleases
303 were removed by purification. After 1% Tx-100 treatment, the minus-strand template remained
304 stable while replication activity was almost completely lost (Fig. 9C) indicating that the detergent
305 sensitivity was not (solely) due to exposure to nucleases but due to solubilization of the
306 membrane-associated RCs.

307 Next, we assessed incorporation of ³²P-CTP into ssRNA, RF and RI by isolating RNA after a
308 replication assay with the purified RCs and treating the isolated RNA with RNases. RF and RI are
309 fully and partially double-stranded RNA molecules, respectively, and under high salt conditions,
310 RNase A/T1 should digest free ssRNA and single-stranded overhangs of RIs and thus the full-length
311 ³²P-labeled RNA observed after the digestion in a denaturing gel is mainly derived from RFs. RNase
312 III should digest RF and double-stranded regions of RIs and after such a treatment, the full-length
313 ³²P-labeled RNA observed in a denaturing gel is mainly derived from ssRNAs. 64% and 19% of the
314 radiolabeled genomic RNA present in the untreated sample was recovered after the RNase A/T1
315 and III treatments in the denaturing electrophoresis, respectively (Fig. 9D). Thus, approximately
316 60% of the newly synthesized RNA was in RF, 20% in RI and 20% in free ssRNAs. However, after
317 both treatments signal might remain that contained an almost full-length ³²P-labeled RNA
318 (annealed with the minus-strand template) or an almost full-length ³²P-labeled single-stranded
319 overhang. Non-denaturing electrophoresis also supported the presence of both RF and RI because
320 the RF/RI signal was reduced approximately 32% after the A/T1 digestion. Most likely single-
321 stranded overhangs in RI were digested and thus the signal was reduced. The untreated and RNase
322 III-treated samples gave equally strong ssRNA signals, whereas after the A/T1 treatment no ssRNA
323 was observed in a non-denaturing gel. The RNase treatments also indicate that SFV replication is
324 semi-conservative because after the A/T1 digestion under high salt conditions, ³²P-labeled
325 genomic RNA was detected in the denaturing gel (Fig. 9D). This is possible only if the labeled RNA
326 was in a dsRNA molecule. If replication were conservative, such a form would not exist.

327 To determine whether the ssRNAs synthesized by the purified RCs were released, we studied
328 their membrane association. For this, the purified RCs were concentrated to remove iodixanol,
329 and after a replication assay pellet and supernatant were separated to detect membrane-

330 associated and free RNA. Most of the ^{32}P -labeled RNA stayed associated with the pellet fraction
331 after the replication assay (Fig. 9E). However, ^{32}P -labeled 26S and 42S RNA were also detected in
332 the supernatant and their amount increased in the same rate in both pellet and supernatant
333 fraction indicating that the more RNA was synthesized, the more RNA was found in the
334 supernatant. At every time point approximately 30% of the labeled genomic RNA was found in the
335 supernatant, which is close to the amount of ssRNA approximated based on the RNase treatments
336 (Fig. 9D and E).

337 Both the presence of newly made RNA in RIs (Fig. 9D) and release of newly made strands
338 (Fig. 9E) indicated that de novo initiation might occur *in vitro*. In addition, the linear rate of RNA
339 synthesis in the unterminated RC samples (Fig. 9A) indicated that the purified RCs might be able to
340 initiate new strands. Thus, we approached this question by determining how much the amount of
341 viral RNA increases during *in vitro* replication compared to the amount of RNA present in the RCs
342 after the purification. We have previously shown that SFV RCs mainly synthesize RNA of positive
343 polarity *in vitro* (39), and thus here we detected plus-strand RNA using a probe that recognizes an
344 early part of the SFV4 genome (nucleotides 95-121). After a 4-h *in vitro* replication assay at 30°C
345 using unlabeled NTPs, RNA was isolated and genomic RNA was detected by in-gel hybridization. In
346 this sample both in-cell made RNA present in the purified RCs as well as *in vitro* synthesized, newly
347 made RNA are detected. For comparison, RNA was also isolated from a reaction, which contained
348 no added NTPs, and from a sample, which contained only purified RCs and was not incubated at
349 30°C. In these samples, only RNA made in cells and present in the purified RCs is detected if we
350 assume that the purified RCs contain no significant amount of cellular NTPs. During *in vitro* RNA
351 synthesis, the amount of completed genomic RNA increased 50% in the active samples compared
352 to the controls without NTPs or without incubation (Fig. 9F). Thus, this result also supports the
353 possibility of de novo initiation during *in vitro* RNA synthesis and, at least, indicates active
354 synthesis of very long RNA stretches resulting in complete genomes.

355 Discussion

356 Our present study demonstrates that the virus-induced plasma membrane invaginations, i.e.
357 spherules, represent the active replication complexes of alphaviruses. We showed here that all
358 four viral nsPs, minus- and plus-strand RNA as well as RNA-synthesizing activity were found in the
359 same purified membrane fraction displaying spherule-like structures on the plasma membrane
360 sheets (Fig. 6-8).

361 Previous purification attempts of alphavirus RCs have mainly focused on the isolation of
362 CPVs (32, 40, 45-47, 50). However, spherules are formed on the plasma membrane and
363 internalization is not typical of all alphaviruses (15, 35, 38). Here, we observed that SFV RCs were
364 most abundant and active when isolated from infected cells treated with wortmannin (Fig. 2),
365 which leads to the retention of the majority of spherules on the plasma membrane (15), and thus
366 we chose to purify spherule-carrying plasma membrane sheets. Firstly, we homogenized cells in
367 isotonic buffer using a needle, instead of hypotonic buffer and a Dounce homogenizer such as
368 used in several previous protocols (32, 40, 41, 45-47). Secondly, we purified RCs from a post-
369 nuclear and -mitochondrial supernatant instead of a membrane pellet (40, 45-47) as differential
370 centrifugation causes a partial loss of activity (Fig. 4) (11, 39). Thirdly, we observed that SFV RCs
371 were sensitive to detergents (Fig. 1F) and thus detergent solubilization was excluded. Fourthly, we
372 used two consecutive density gradients of iodixanol under isotonic conditions. Our purification
373 protocol yielded RCs that were highly active in synthesizing both genomic and subgenomic RNA as
374 well as released newly made strands (Fig. 9). In addition, our purification method produced highly
375 active complexes in large quantities as from $\sim 10^7$ cells, we purified enough RCs to make at least
376 one hundred standard *in vitro* replication assays, and it can easily be further scaled up.

377 The sedimentation analyses revealed that SFV infection extensively modifies cellular
378 membranes (Fig. 5). The plasma membrane had higher density, most likely due to the RNA-
379 containing RCs. Furthermore, major differences in three ER markers were observed and the ER
380 showed increased density after infection, indicating that SFV may cause ER re-modelling. Several
381 viruses are known to affect ER organization. For example herpes simplex virus 1 (HSV-1) infection
382 results in compression of ER around the nuclear membrane, most likely to facilitate nuclear egress
383 of HSV-1 nucleocapsids (51). SFV infection also affected the late endosomal and lysosomal
384 markers. Consequently, SFV has more profound effects on the membrane dynamics of the host
385 cell than merely inducing plasma membrane invaginations.

Purification of the RCs resulted in a replication-active membrane fraction enriched with the markers for the plasma membrane, ER and late endosomes (Fig. 6). We could remove soluble proteins, the Golgi, and most of the mitochondria. The corresponding membrane fraction from mock cells revealed only a minor signal for the ER marker calnexin indicating that we purified a virus-specific network of membranes associated with replication. In cells, the peripheral ER tubules form a branched network contacting the cytoskeleton, plasma membrane and cell organelles (52). The purified membrane preparations revealed ER markers for both ER sheets and tubules, although the marker used for the ER sheets has been reported to be found also at the plasma membrane (48). However, it remains to be studied if the RC-carrying plasma membrane sheets are truly connected to the other membranes or if these membranes have the same density. Clearly, this enrichment was not observed in the mock samples, and thus, SFV infection modified the studied membranes. However, besides genome replication, expression of SFV structural proteins and host defense responses may affect different membranes. Another possibility is that SFV infection causes the re-localization of some cellular proteins. For example the late endosomal marker Rab7 was present in the purified RC-membrane fraction, but the endo-lysosomal marker LAMP-2 could not be detected and thus Rab7 could have been re-localized during infection.

Membrane association of the replicase proteins, mediated mainly by nsP1, is indispensable for alphaviruses (25, 53, 54), and our results showed that detergent solubilization caused a significant loss of replication activity although the minus-strand template was stable (Fig. 1F and 9C). Thus, the polymerase activity was sensitive to detergents further highlighting the importance of the membrane association of the RCs. Detergent solubilization has, however, been shown to increase the density of alphaviral RCs while they retain all nsPs and residual RNA synthesis activity (45). It remains to be studied whether the membrane association of SFV nsPs occurs only in the spherule neck or if they are also found inside the membrane invagination. Cryo-electron tomography of Flock house nodavirus (FHV) spherules has revealed a crown structure in the spherule neck with a 12-fold symmetry and a central electron density (12). It was suggested that FHV replicase protein A forms these structures, and if alphavirus RCs establish a similar structure, it may have a different organization as alphaviruses have four replicase proteins instead of one.

We observed that the purified RCs incorporated ³²P-CTP into both ssRNA and dsRNA and released newly made RNA (Fig. 9), and approximately 20-30% of the newly made genomic RNA was released as ssRNA. This data indicated that de novo initiation might occur *in vitro*. Secondly, we determined that the amount of genomic RNA present in the purified RCs was increased ~1.5

418 times during the *in vitro* replication. As the probe used recognizes an early part of the genome, the
419 results indicate that long RNA strands were produced *in vitro* and consequently most *in vitro*
420 synthesized strands were either de novo initiated or were re-initiated from a short RNA made in
421 cells. Furthermore, the results also showed that high amounts of RNA was produced *in vitro*. So
422 far, it is unclear how many copies of genomic RNA SFV spherules contain. FHV spherules are
423 variable in size and the authors speculate that some spherules may contain more than one dsRNA
424 or positive-strand RNA (12).

425 In PNS, most of the *in vitro* synthesized RNA is single stranded (11, 40), and *in vitro*
426 synthesized RF and RI reach the maximal level in about 15 min after which only the amount of
427 ssRNA increases (55). In alphavirus-infected mammalian cells, CPVs are located close to the
428 ribosome-rich ER and connecting bridges are formed that may represent RNA strands being
429 translated. The release of the newly made RNA might thus require translation or nucleocapsid
430 assembly and it has been suggested that these occur in a matrix between CPVs and the rough ER
431 (36, 56). If the efficient release of the newly made RNA strands requires translation and assembly
432 of the nucleocapsids close to the RCs, this may explain why most of the *in vitro*-synthesized RNA
433 remained in membrane-associated, double-stranded replicative forms or intermediates. Although
434 we observed SFV capsid protein and nucleocapsids in the purified membrane fraction (Fig. 6 and
435 8), efficient encapsidation may not be achieved *in vitro* using purified membranes as no ribosomal
436 RNA was detected.

437 In conclusion, we showed that alphavirus infection strongly modifies cellular membranes
438 beyond inducing the spherules and that the ER might be connected to the RC-carrying plasma
439 membrane. This is the first step forward in extending our knowledge of alphavirus membrane-
440 associated RCs and further studies on these purified complexes should give insights into the host
441 proteins present and required for their activity on the plasma membrane, as well as their
442 structural organization. Currently, alphaviruses, coronaviruses and arteriviruses represent
443 important groups of pathogenic positive-strand RNA viruses lacking structural information on
444 RdRps (57, 58). The alphaviral core RdRp has been purified in an active form (31) but the structure
445 of the RC might give more information about the active conformation of the polymerase and
446 interactions, as all four nsPs are required for RNA synthesis.

447 **Materials and Methods**

448

449 **Cell culture, viruses and plasmids**

450 BHK-21 cells were maintained in Dulbecco's modified Eagle's medium (DMEM; Sigma-Aldrich)
451 supplemented with 10% (v/v) fetal bovine serum (FBS; Gibco), 2 mM L-glutamine (Gibco), 100
452 U/ml penicillin (Gibco), and 100 µg/ml streptomycin (Gibco). BSR T7/5 cells, a derivative of BHK
453 stably expressing T7 RNA polymerase (59), were cultured in DMEM supplemented with 10% FBS,
454 2% (v/v) tryptose phosphate broth (Difco), 2 mM L-glutamine, 1% (v/v) non-essential amino acids
455 (Gibco), 1 mg/ml G418 (Merck), 100 U/ml penicillin, and 100 µg/ml streptomycin. Both cell lines
456 were grown at 37°C and in 5% CO₂. The same conditions were used for virus infection and DNA
457 transfection. SFV4-HA, containing a hemagglutinin (HA) peptide in frame within nsP3 in XhoI site,
458 has been described and was propagated as previously (39). Secondary stocks of SFV4-HA were
459 used in all virus infections. The polyprotein construct P123^{HA}4 and template Tmed have been
460 described previously (39, 60).

461

462 **Isolation of RCs from infected and transfected cells**

463 About 1×10⁷ BHK-21 cells were infected with SFV4-HA at a MOI of 50 or 500 for 1 h or 20 min,
464 respectively, in MEM containing 0.2% BSA and 2 mM L-glutamine. After the adsorption, cells were
465 washed twice and fresh medium was added. Wortmannin (100 nm; Sigma-Aldrich) and nocodazole
466 (5 µM; Calbiochem) treatments were performed as described previously (15). Nocodazole was
467 added at the same time as the virus and Wortmannin at 1.5 h p.i. Cells were harvested at 4 h p.i.
468 by trypsinization and PNS was prepared using a Dounce homogenizer as described in (39). BSR
469 cells were co-transfected with the polyprotein and Tmed template plasmids and 16 h after
470 transfection PNS and P15 membrane fractions were prepared as previously described (39).

471

472 **Purification of RCs from infected cells**

473 Approximately 4×10⁷ BHK-21 cells were infected with SFV4-HA at a MOI of 500 and treated with
474 wortmannin as above. Mock-infected cells served as a control and were treated with wortmannin.
475 At 4 h p.i., cells were harvested by scraping in phosphate-buffered saline and washed with
476 homogenization buffer (HB) [250 mM sucrose, 3 mM imidazole (pH 7.4), 2 µg/ml Actinomycin D
477 (Sigma-Aldrich), Pierce EDTA-Free Protease Inhibitor (1 tablet per 10 ml; Thermo Fisher Scientific)]
478 and resuspended in 500 µl of HB containing 200 U/ml RiboLock (Thermo Fisher Scientific). Cells

479 were disrupted using a 22-G needle and syringe by 24 up-and-down strokes. Unlysed cells and
480 nuclei were removed by centrifugation ($510 \times g$, 10 min, 4°C) yielding PNS which was diluted 3-fold
481 with HB containing RiboLock. Membrane pellet (P7) and soluble fraction (S7) were prepared by
482 further centrifugation of the diluted PNS ($7,000 \times g$, 10 min, 4°C). The P7 fraction was washed once
483 with and resuspended in HB containing RiboLock.

484 RCs were purified from S7 fractions by sedimentation ($100,000 \times g$, 3 h, 4°C) in a
485 discontinuous iodixanol (Sigma-Aldrich) gradient consisting of 2.3-ml layers of 20, 17.5, 15, 12.5,
486 and 10% (w/v) iodixanol in dilution buffer (DB) [250 mM sucrose, 35 mM HEPES (pH 7.4), 2.5 mM
487 DTT, 7 mM KCl] containing Pierce EDTA-Free Protease Inhibitor (1 tablet per 10 ml). 500 μl of S7
488 was loaded on the top of a gradient. After sedimentation, gradients were fractionated and protein,
489 lipid and RNA composition as well as replication activity were analyzed as described below.
490 Density of the fractions was measured by weighing. For further purification, the light-scattering
491 zone between 12.5% and 15% iodixanol layers was collected and purified by equilibrium flotation
492 centrifugation ($90,000 \times g$, 18 h, 4°C) in a discontinuous iodixanol gradient consisting of 3 ml of
493 30% and 1.8-ml layers of 26, 22, 18, 14, and 10% (w/v) iodixanol in DB. 30% layer contained the
494 light-scattering zone collected from the sedimentation gradient. After flotation, gradients were
495 fractionated and fractions analyzed as the sedimentation fractions. For further experiments, the
496 light-scattering zone between 14% and 18% iodixanol layers was collected yielding purified RCs. As
497 a control, membranes from wortmannin-treated mock-infected cells were purified using the same
498 protocol.

499

500 ***In vitro* replication assays**

501 A standard 30- μl reaction without BSA contained 25 μl of PNS, 32 mM HEPES (pH 7.4), 225 mM
502 sucrose, 2.3 mM DTT, 6.3 mM KCl, 1.7 $\mu\text{g/ml}$ Actinomycin D, and 830 U/ml RiboLock. A standard
503 30- μl reaction with BSA contained 22 μl of PNS, S7, P7, P15, sedimentation or flotation fractions,
504 or purified RCs, 1 mg/ml BSA, 28 mM HEPES (pH 7.4), 200 mM sucrose, 2 mM DTT, 5.6 mM KCl, 1.5
505 $\mu\text{g/ml}$ Actinomycin D, and 810 U/ml RiboLock. In addition, both reactions contained 3 mM
506 magnesium acetate, 17 mM creatine phosphate (Sigma-Aldrich), 8.3 U/ml creatine phosphokinase
507 (Sigma-Aldrich), 1 mM ATP, 10 μM UTP, 10 μM GTP, 8.5 μM CTP, and 0.055 μM (5 μCi) of α - ^{32}P -
508 CTP (Perkin Elmer). If required, samples were diluted with DB, and if samples contained imidazole,
509 6 mM magnesium acetate was used in the reaction mixture. Reactions were incubated at 30°C for
510 1 h unless otherwise stated. After incubation, reactions were terminated by adding LiDS/LET [5%

511 lithium dodecyl sulfate, 20 mM Tris-HCl (pH 7.4), 100 mM LiCl, 2 mM EDTA, and 5 mM DTT]
512 containing 80 µg/ml proteinase K and incubating for 15 min at 37°C. Unincorporated label was
513 removed using RNase-free Micro Bio-Spin™ P-30 Gel Columns (Bio-rad), and acid phenol method
514 was used to isolate RNA.

515 To determine stability of RCs, PNS was incubated at 4°C for 3, 24 and 48 or diluted in DB or
516 35.5% (w/v) iodixanol in DB and incubated at 4°C for 24 h. After incubation, aliquots were
517 removed for total RNA isolation and in-gel hybridization to detect endogenous RNA (see below)
518 and for an *in vitro* replication assay. To test detergent sensitivity, PNS was treated with 0.01-1% n-
519 Octylglucoside (w/v), Tx-100 (v/v), DOC (w/v), or SDS (w/v) in DB at 4°C for 1 h, followed by total
520 RNA isolation and in-gel hybridization to detect endogenous RNA (see below) or a replication
521 assay. To inhibit replication, 100 µM 3'-dCTP (TriLink BioTechnologies) was added to the reaction
522 mixture.

523 To follow the stability of newly synthesized RNA in the S7 fraction or purified RCs, 100 µM 3'-
524 dCTP and 220 ng of Tmed *in vitro* transcript were added in one aliquot and DB to another one
525 after a 1-h replication assay. *In vitro* transcript was prepared using a SacI-linearized Tmed plasmid
526 and mMMESSAGE mMACHINE® T7 Transcription Kit (Ambion) according to manufacturer's
527 instructions. After a chase at 30°C, aliquots were removed and reactions were terminated as
528 described above.

529 Ability of RCs to use an exogenous template RNA was tested by adding 1 µg of Tmed *in vitro*
530 transcript in a reaction mixture containing purified RCs. As a control, P15 from cells transfected
531 with the polyprotein P123^{HA}4 and template Tmed plasmids was used. Replication assay reactions
532 were incubated at 30°C for 2 h and terminated as described above. In order to test Tx-100
533 sensitivity of purified RCs, they were incubated with 1% Tx-100 for 1 h at 25°C. After incubation,
534 aliquots were removed for total RNA isolation and in-gel hybridization to detect endogenous RNA
535 (see below) or a replication assay.

536 In order to determine how much the amount of genomic RNA increases during *in vitro*
537 replication compared to the amount of genomic RNA present in the RCs after purification,
538 replication assays were performed using purified RCs and reaction conditions described above for
539 a standard reaction with BSA, except for that 10 µM CTP and no α-³²P-CTP were used. In addition,
540 a reaction devoid of NTPs was performed. After a 4-h incubation at 30°C, RNA was isolated and
541 genomic RNA was detected by in-gel hybridization (see below). As a control, RNA was isolated
542 from the purified RCs without incubation at 30°C.

543

544 **RNA isolation, denaturing agarose gel electrophoresis and in-gel hybridization**

545 Total RNA from replication assay reactions, PNS, S7, and P7 samples, sedimentation and flotation
546 fractions, and purified RCs was isolated using the acid phenol method and analysed by denaturing
547 formaldehyde agarose gel electrophoresis as described previously (39). If required, spike RNA
548 (Tmed or Tshort *in vitro* transcript) was added in the samples before RNA isolation to allow
549 normalization. Tshort *in vitro* transcript was prepared from the Tshort plasmid (60) as described
550 above for Tmed.

551 In-gel hybridization to detect RNA molecules from dried gels using ³²P-labeled
552 oligonucleotides has been described previously (61). SFV4-HA negative-stranded RNA was
553 detected with the probe HybSFV4neg_4 and genomic and subgenomic RNA were detected with
554 the probe HybSFV4pos_5 (39). SFV4-HA genomic RNA and RNA II were detected with the probe
555 HybSFV4pos_8 (5'-GTCAGCCTCAATATCAACATGCACTTT-3') complementary to nucleotides 95-121
556 of the genome. Tmed RNA was detected with the probe HybTmedpos_2 (39). Tshort RNA was
557 detected with the probe HybTmedpos_3 (5'-AGGTGTATAACAGGTCCTCTCATTAATT-3')
558 complementary to nucleotides 1,270-1,297. 18S rRNA was detected with the probe 5'-
559 ATGCCCCCGGCCGTCCCTCT-3'.

560 Dried gels were exposed to Phosphor Imager screens to detect ³²P-label, and the screens
561 were scanned with a Typhoon 9410 imager (GE Healthcare). Quantity One software (Bio-rad) was
562 used to quantify the incorporated label. Normalization of signals for variations in RNA recovery
563 and loading was done based on quantification of 18S rRNA or spike RNA detected by in-gel
564 hybridization.

565

566 **RNase treatments of products from an *in vitro* replication assay**

567 Replication assays were performed using purified RCs and 2-h reaction time and RNA was isolated
568 as described above. Isolated RNA was treated with RNase Cocktail™ Enzyme Mix (Ambion)
569 containing RNase A and T1 (final concentrations of 2.5 and 100 U/ml, respectively) or RNase III (50
570 U/ml; NEBNext RNase III RNA Fragmentation module) under high salt conditions. RNase A/T1
571 reaction contained 4×SSC (600 mM NaCl, 60 mM sodium citrate, pH 7.0) and RNase III reaction
572 2×SSC (300 mM NaCl, 30 mM sodium citrate, pH 7.0) and 1× RNase III reaction buffer. After a 15-
573 min incubation at 37°C, proteinase K was added (80 µg/ml) and incubation was continued for 15
574 min. RNA was precipitated as described in (39). Besides denaturing formaldehyde agarose gel

575 electrophoresis, RNA was analysed without denaturation in a 1.0% (w/v) agarose gel in Tris-
576 Borate-EDTA buffer after mixing with 2 volumes of Gel Loading Buffer II (Ambion).

577

578 **RNA release**

579 To study release of newly synthesized RNA, purified RCs were concentrated and iodixanol was
580 removed by washing with DB in Amicon Ultra Centrifugal Filter Units (Merck Millipore; 50,000
581 nominal molecular weight limit; $3,220 \times g$, 4°C). An *in vitro* replication assay was performed as
582 described above and after 1, 2 and 3-h reaction time, aliquots were removed, diluted with DB and
583 pellet and supernatant fractions were separated by differential centrifugation ($20,600 \times g$, 15 min,
584 4°C). The pellet was washed with DB, and the pellet and supernatant were treated with proteinase
585 K (80 µg/ml) for 15 min at 37°C. RNA was isolated using the acid phenol method (39).

586

587 **Protein and lipid analyses**

588 Protein concentrations were measured using the Coomassie blue method (62), with BSA as a
589 standard. PNS, S7, P7 and sedimentation and flotation fractions were analysed by SDS-
590 polyacrylamide gel electrophoresis (SDS-PAGE) with 4% (w/v) acrylamide concentration in the
591 stacking and 10%, 12% or 16% (w/v) acrylamide concentration in the separation gel. 12% SDS-
592 PAGE gels were stained with Coomassie blue to show proteins. 16% SDS-PAGE gels were stained
593 with Sudan Black B (Sigma-Aldrich) according to manufacturer's instructions to detect lipids. After
594 electrophoresis, Sudan Black B stains both lipids and lipoproteins. For Western blotting, proteins
595 separated in 10% or 12% SDS-PAGE gels were transferred to AmershamTM ProtanTM Nitrocellulose
596 Blotting Membrane (GE Healthcare). Membranes were blocked with 5% (w/v) non-fat dry milk
597 powder in Tris-buffered saline (TBS) followed by incubation with rabbit polyclonal antibodies
598 against SFV nsP1, nsP2, nsP3, or nsP4 (37) or mouse monoclonal antibody against β -actin (Sigma-
599 Aldrich) in TBS with 5% milk and 0.1% (v/v) Tween-20. Alternatively, membranes were blocked
600 with 5% milk in TBS containing 0.1% Tween-20 followed by incubation with rabbit monoclonal
601 antibody against SDHA (Cell Signaling), mouse monoclonal antibody against PMCA (Abcam), rabbit
602 polyclonal antibody against Na,K-ATPase α (Cell Signaling), rabbit polyclonal antibody against
603 calnexin (Abcam), rabbit polyclonal antibody against CLIMP-63 (Abcam), rabbit polyclonal antibody
604 against RTN4A and RTN4B (Abcam), mouse monoclonal antibody against GM130 (BD Biosciences),
605 mouse monoclonal antibody against Rab7 (Abcam), rabbit polyclonal antibody against LAMP-2
606 (Novus Biologicals), or rabbit polyclonal antibody against SFV capsid protein (63) in TBS with 5%

607 (w/v) BSA and 0.1% Tween-20. The primary antibodies were detected with secondary antibodies
608 IRDye®800CW donkey anti-rabbit IgG (Li-COR Biosciences) or Alexa Fluor 680 donkey anti-mouse
609 IgG (Invitrogen) and Odyssey system (Li-cor). Quantification was performed with Image Studio
610 Software (Li-COR). The antibody against RTN4A and RTN4B recognized only a band of about 50 kDa
611 (49) indicating that the detected protein was RTN4B, and the result was confirmed using sheep
612 polyclonal antibody against RTN4B (MRCPPUreagents).

613

614 **Electron microscopy**

615 The light-scattering zone between 14% and 18% iodixanol layers in the flotation gradient (see
616 purification above) was collected and fixed with 2% (v/v) glutaraldehyde (Sigma-Aldrich) in 100
617 mM HEPES (pH 7.4) on ice for 30 min. After fixation, membranes were pelleted by differential
618 centrifugation ($11,700 \times g$, 30 min, 4°C). Membrane pellets were washed, osmicated and
619 embedded into resin (TAAB) using standard procedures and ultra-thin sections (60 nm) were cut,
620 picked on single slot copper grids and post stained with lead and uranyl acetate. The homogeneity
621 of the pellet was checked by systematic sectioning through the entire pellet. The micrographs
622 were taken with a Jeol JEM-1400 transmission electron microscope operating at 80 kV at the
623 Electron Microscopy Unit of the Institute of Biotechnology, University of Helsinki.

624 **Acknowledgments**

625 We thank Dr Eija Jokitalo for valuable discussions and Arja Välimäki, Mika Lång and Ilkka Kivistö for
626 excellent technical assistance. The authors acknowledge the support and the use of resources of
627 Centre for Virus and Macromolecular Complex Production (ICVIR, University of Helsinki), part of
628 Instruct-FI.

629 This work was supported by a three-year research project grant of the University of Helsinki
630 (M.K.P.), an Academy of Finland Postdoctoral Researcher grant (274748; M.K.P.) and Academy of
631 Finland Project grants (265997 and 307802; T.A.).

632 References

- 633 1. Yang X, Yang H, Zhou G, Zhao GP. 2008. Infectious disease in the genomic era. *Annu Rev Genomics*
634 *Hum Genet* 9:21-48.
- 635 2. Koonin EV, Dolja VV, Krupovic M. 2015. Origins and evolution of viruses of eukaryotes: The ultimate
636 modularity. *Virology* 479-480:2-25.
- 637 3. Strauss JH, Strauss EG. 1994. The alphaviruses: gene expression, replication, and evolution.
638 *Microbiol Rev* 58:491-562.
- 639 4. den Boon JA, Ahlquist P. 2010. Organelle-like membrane compartmentalization of positive-strand
640 RNA virus replication factories. *Annu Rev Microbiol* 64:241-56.
- 641 5. Paul D, Bartenschlager R. 2013. Architecture and biogenesis of plus-strand RNA virus replication
642 factories. *World J Virol* 2:32-48.
- 643 6. Salonen A, Ahola T, Kääriäinen L. 2005. Viral RNA replication in association with cellular
644 membranes. *Curr Top Microbiol Immunol* 285:139-73.
- 645 7. Knoops K, Kikkert M, Worm SH, Zevenhoven-Dobbe JC, van der Meer Y, Koster AJ, Mommaas AM,
646 Snijder EJ. 2008. SARS-coronavirus replication is supported by a reticulovesicular network of
647 modified endoplasmic reticulum. *PLoS Biol* 6:e226.
- 648 8. Knoops K, Barcena M, Limpens RW, Koster AJ, Mommaas AM, Snijder EJ. 2012. Ultrastructural
649 characterization of arterivirus replication structures: reshaping the endoplasmic reticulum to
650 accommodate viral RNA synthesis. *J Virol* 86:2474-87.
- 651 9. Limpens RW, van der Schaar HM, Kumar D, Koster AJ, Snijder EJ, van Kuppeveld FJ, Barcena M.
652 2011. The transformation of enterovirus replication structures: a three-dimensional study of single-
653 and double-membrane compartments. *MBio* 2.
- 654 10. Romero-Brey I, Merz A, Chiramel A, Lee JY, Chlanda P, Haselman U, Santarella-Mellwig R,
655 Habermann A, Hoppe S, Kallis S, Walther P, Antony C, Krijnse-Locker J, Bartenschlager R. 2012.
656 Three-dimensional architecture and biogenesis of membrane structures associated with hepatitis C
657 virus replication. *PLoS Pathog* 8:e1003056.
- 658 11. Albulescu IC, Tas A, Scholte FE, Snijder EJ, van Hemert MJ. 2014. An in vitro assay to study
659 chikungunya virus RNA synthesis and the mode of action of inhibitors. *J Gen Virol* 95:2683-92.
- 660 12. Ertel KJ, Benefield D, Castano-Diez D, Pennington JG, Horswill M, den Boon JA, Otegui MS, Ahlquist
661 P. 2017. Cryo-electron tomography reveals novel features of a viral RNA replication compartment.
662 *Elife* 6.
- 663 13. Kallio K, Hellström K, Balistreri G, Spuul P, Jokitalo E, Ahola T. 2013. Template RNA length
664 determines the size of replication complex spherules for Semliki Forest virus. *J Virol* 87:9125-34.
- 665 14. Kopeck BG, Perkins G, Miller DJ, Ellisman MH, Ahlquist P. 2007. Three-dimensional analysis of a viral
666 RNA replication complex reveals a virus-induced mini-organelle. *PLoS Biol* 5:e220.
- 667 15. Spuul P, Balistreri G, Kääriäinen L, Ahola T. 2010. Phosphatidylinositol 3-kinase-, actin-, and
668 microtubule-dependent transport of Semliki Forest Virus replication complexes from the plasma
669 membrane to modified lysosomes. *J Virol* 84:7543-57.
- 670 16. Schwartz M, Chen J, Janda M, Sullivan M, den Boon J, Ahlquist P. 2002. A positive-strand RNA virus
671 replication complex parallels form and function of retrovirus capsids. *Mol Cell* 9:505-14.
- 672 17. Ryman KD, Klimstra WB. 2008. Host responses to alphavirus infection. *Immunol Rev* 225:27-45.
- 673 18. Schilte C, Staikowsky F, Couderc T, Madec Y, Carpentier F, Kassab S, Albert ML, Lecuit M, Michault
674 A. 2013. Chikungunya virus-associated long-term arthralgia: a 36-month prospective longitudinal
675 study. *PLoS Negl Trop Dis* 7:e2137.
- 676 19. Khan AH, Morita K, Parquet Md Mdel C, Hasebe F, Mathenge EG, Igarashi A. 2002. Complete
677 nucleotide sequence of chikungunya virus and evidence for an internal polyadenylation site. *J Gen*
678 *Virol* 83:3075-84.
- 679 20. Lemm JA, Rumenapf T, Strauss EG, Strauss JH, Rice CM. 1994. Polypeptide requirements for
680 assembly of functional Sindbis virus replication complexes: a model for the temporal regulation of
681 minus- and plus-strand RNA synthesis. *EMBO J* 13:2925-34.

- 682 21. Shirako Y, Strauss JH. 1994. Regulation of Sindbis virus RNA replication: uncleaved P123 and nsP4
683 function in minus-strand RNA synthesis, whereas cleaved products from P123 are required for
684 efficient plus-strand RNA synthesis. *J Virol* 68:1874-85.
- 685 22. Ahola T, Kääriäinen L. 1995. Reaction in alphavirus mRNA capping: formation of a covalent complex
686 of nonstructural protein nsP1 with 7-methyl-GMP. *Proc Natl Acad Sci U S A* 92:507-11.
- 687 23. Lemm JA, Rice CM. 1993. Roles of nonstructural polyproteins and cleavage products in regulating
688 Sindbis virus RNA replication and transcription. *J Virol* 67:1916-26.
- 689 24. Lemm JA, Rice CM. 1993. Assembly of functional Sindbis virus RNA replication complexes:
690 requirement for coexpression of P123 and P34. *J Virol* 67:1905-15.
- 691 25. Spuul P, Salonen A, Merits A, Jokitalo E, Kaariainen L, Ahola T. 2007. Role of the amphipathic
692 peptide of Semliki forest virus replicase protein nsP1 in membrane association and virus
693 replication. *J Virol* 81:872-83.
- 694 26. Das PK, Merits A, Lulla A. 2014. Functional cross-talk between distant domains of chikungunya virus
695 non-structural protein 2 is decisive for its RNA-modulating activity. *J Biol Chem* 289:5635-53.
- 696 27. Hardy WR, Strauss JH. 1989. Processing the nonstructural polyproteins of sindbis virus:
697 nonstructural proteinase is in the C-terminal half of nsP2 and functions both in cis and in trans. *J*
698 *Virol* 63:4653-64.
- 699 28. Vasiljeva L, Merits A, Golubtsov A, Sizemskaja V, Kaariainen L, Ahola T. 2003. Regulation of the
700 sequential processing of Semliki Forest virus replicase polyprotein. *J Biol Chem* 278:41636-45.
- 701 29. Kim DY, Reynaud JM, Rasalouslykaya A, Akhrymuk I, Mobley JA, Frolov I, Frolova EI. 2016. New World
702 and Old World Alphaviruses Have Evolved to Exploit Different Components of Stress Granules, FXR
703 and G3BP Proteins, for Assembly of Viral Replication Complexes. *PLoS Pathog* 12:e1005810.
- 704 30. Li C, Debing Y, Jankevicius G, Neyts J, Ahel I, Coutard B, Canard B. 2016. Viral Macro Domains
705 Reverse Protein ADP-Ribosylation. *J Virol* 90:8478-86.
- 706 31. Rubach JK, Wasik BR, Rupp JC, Kuhn RJ, Hardy RW, Smith JL. 2009. Characterization of purified
707 Sindbis virus nsP4 RNA-dependent RNA polymerase activity in vitro. *Virology* 384:201-8.
- 708 32. Friedman RM, Levin JG, Grimley PM, Berezesky IK. 1972. Membrane-associated replication complex
709 in arbovirus infection. *J Virol* 10:504-15.
- 710 33. Grimley PM, Berezesky IK, Friedman RM. 1968. Cytoplasmic structures associated with an arbovirus
711 infection: loci of viral ribonucleic acid synthesis. *J Virol* 2:1326-38.
- 712 34. Grimley PM, Levin JG, Berezesky IK, Friedman RM. 1972. Specific membranous structures
713 associated with the replication of group A arboviruses. *J Virol* 10:492-503.
- 714 35. Frolova EI, Gorchakov R, Pereboeva L, Atasheva S, Frolov I. 2010. Functional Sindbis virus replicative
715 complexes are formed at the plasma membrane. *J Virol* 84:11679-95.
- 716 36. Froshauer S, Kartenbeck J, Helenius A. 1988. Alphavirus RNA replicase is located on the cytoplasmic
717 surface of endosomes and lysosomes. *J Cell Biol* 107:2075-86.
- 718 37. Kujala P, Ikäheimonen A, Ehsani N, Vihinen H, Auvinen P, Kääriäinen L. 2001. Biogenesis of the
719 Semliki Forest virus RNA replication complex. *J Virol* 75:3873-84.
- 720 38. Thaa B, Biasiotto R, Eng K, Neuvonen M, Gotte B, Rheinemann L, Mutso M, Utt A, Varghese F,
721 Balistreri G, Merits A, Ahola T, McInerney GM. 2015. Differential Phosphatidylinositol-3-Kinase-Akt-
722 mTOR Activation by Semliki Forest and Chikungunya Viruses Is Dependent on nsP3 and Connected
723 to Replication Complex Internalization. *J Virol* 89:11420-37.
- 724 39. Pietilä MK, Albulescu IC, Hemert MJV, Ahola T. 2017. Polyprotein Processing as a Determinant for in
725 Vitro Activity of Semliki Forest Virus Replicase. *Viruses* 9.
- 726 40. Clewley JP, Kennedy SI. 1976. Purification and polypeptide composition of Semliki Forest virus RNA
727 polymerase. *J Gen Virol* 32:395-411.
- 728 41. Sreevalsan T, Yin FH. 1969. Sindbis virus-induced viral ribonucleic acid polymerase. *J Virol* 3:599-
729 604.
- 730 42. Wielgosz MM, Huang HV. 1997. A novel viral RNA species in Sindbis virus-infected cells. *J Virol*
731 71:9108-17.

- 732 43. van Hemert MJ, de Wilde AH, Gorbalenya AE, Snijder EJ. 2008. The in vitro RNA synthesizing activity
733 of the isolated arterivirus replication/transcription complex is dependent on a host factor. *J Biol*
734 *Chem* 283:16525-36.
- 735 44. van Hemert MJ, van den Worm SH, Knoop K, Mommaas AM, Gorbalenya AE, Snijder EJ. 2008.
736 SARS-coronavirus replication/transcription complexes are membrane-protected and need a host
737 factor for activity in vitro. *PLoS Pathog* 4:e1000054.
- 738 45. Barton DJ, Sawicki SG, Sawicki DL. 1991. Solubilization and immunoprecipitation of alphavirus
739 replication complexes. *J Virol* 65:1496-506.
- 740 46. Gomatos PJ, Kääriäinen L, Keränen S, Ranki M, Sawicki DL. 1980. Semliki Forest virus replication
741 complex capable of synthesizing 42S and 26S nascent RNA chains. *J Gen Virol* 49:61-9.
- 742 47. Ranki M, Kääriäinen L. 1979. Solubilized RNA replication complex from Semliki Forest virus-infected
743 cells. *Virology* 98:298-307.
- 744 48. Sandoz PA, van der Goot FG. 2015. How many lives does CLIMP-63 have? *Biochem Soc Trans*
745 43:222-8.
- 746 49. Rämö O, Kumar D, Gucciardo E, Joensuu M, Saarekas M, Vihinen H, Belevich I, Smolander OP, Qian
747 K, Auvinen P, Jokitalo E. 2016. NOGO-A/RTN4A and NOGO-B/RTN4B are simultaneously expressed
748 in epithelial, fibroblast and neuronal cells and maintain ER morphology. *Sci Rep* 6:35969.
- 749 50. Varjak M, Saul S, Arike L, Lulla A, Peil L, Merits A. 2013. Magnetic fractionation and proteomic
750 dissection of cellular organelles occupied by the late replication complexes of Semliki Forest virus. *J*
751 *Virol* 87:10295-312.
- 752 51. Maeda F, Arai J, Hirohata Y, Maruzuru Y, Koyanagi N, Kato A, Kawaguchi Y. 2017. Herpes Simplex
753 Virus 1 UL34 Protein Regulates the Global Architecture of the Endoplasmic Reticulum in Infected
754 Cells. *J Virol* 91.
- 755 52. Phillips MJ, Voeltz GK. 2016. Structure and function of ER membrane contact sites with other
756 organelles. *Nat Rev Mol Cell Biol* 17:69-82.
- 757 53. Ahola T, Lampio A, Auvinen P, Kääriäinen L. 1999. Semliki Forest virus mRNA capping enzyme
758 requires association with anionic membrane phospholipids for activity. *EMBO J* 18:3164-72.
- 759 54. Salonen A, Vasiljeva L, Merits A, Magden J, Jokitalo E, Kääriäinen L. 2003. Properly folded
760 nonstructural polyprotein directs the semliki forest virus replication complex to the endosomal
761 compartment. *J Virol* 77:1691-702.
- 762 55. Michel MR, Gomatos PJ. 1973. Semliki forest virus-specific RNAs synthesized in vitro by enzyme
763 from infected BHK cells. *J Virol* 11:900-14.
- 764 56. Jose J, Taylor AB, Kuhn RJ. 2017. Spatial and Temporal Analysis of Alphavirus Replication and
765 Assembly in Mammalian and Mosquito Cells. *MBio* 8.
- 766 57. Pietilä MK, Hellström K, Ahola T. 2017. Alphavirus polymerase and RNA replication. *Virus Res*
767 234:44-57.
- 768 58. Posthuma CC, Te Velhuis AJW, Snijder EJ. 2017. Nidovirus RNA polymerases: Complex enzymes
769 handling exceptional RNA genomes. *Virus Res* 234:58-73.
- 770 59. Buchholz UJ, Finke S, Conzelmann KK. 1999. Generation of bovine respiratory syncytial virus (BRSV)
771 from cDNA: BRSV NS2 is not essential for virus replication in tissue culture, and the human RSV
772 leader region acts as a functional BRSV genome promoter. *J Virol* 73:251-9.
- 773 60. Spuul P, Balistreri G, Hellström K, Golubtsov AV, Jokitalo E, Ahola T. 2011. Assembly of alphavirus
774 replication complexes from RNA and protein components in a novel trans-replication system in
775 mammalian cells. *J Virol* 85:4739-51.
- 776 61. Scholte FE, Tas A, Martina BE, Cordioli P, Narayanan K, Makino S, Snijder EJ, van Hemert MJ. 2013.
777 Characterization of synthetic Chikungunya viruses based on the consensus sequence of recent E1-
778 226V isolates. *PLoS One* 8:e71047.
- 779 62. Bradford MM. 1976. A rapid and sensitive method for the quantitation of microgram quantities of
780 protein utilizing the principle of protein-dye binding. *Anal Biochem* 72:248-54.
- 781 63. Väänänen P, Kääriäinen L. 1979. Haemolysis by two alphaviruses: Semliki Forest and Sindbis virus. *J*
782 *Gen Virol* 43:593-601.

Figures and figure legends

Figure 1. SFV RCs are stable and robust in RNA synthesis *in vitro*. (A) BHK cells were infected with SFV at a MOI of 50 and PNS was prepared at 4 h p.i. *In vitro* replication was studied by the incorporation of ^{32}P -CTP into SFV RNA indicated by 26S, II and 42S. After the incubation times indicated, RNA was isolated and analysed in a denaturing agarose gel. Ribosomal 18S RNA (18S rRNA) was detected by in-gel hybridization from the same gel. (B) Kinetics of the incorporation of ^{32}P -CTP into 26S (blue) and 42S (green) RNA. Percentages indicate the incorporation compared to the last time point (100%). Data are presented as means \pm standard deviation from two independent experiments. (C) Replication assay performed with either undiluted PNS or PNS diluted as indicated. 18S rRNA was detected as in A. For the undiluted sample, 1/10th of RNA was loaded compared to the others. (D) Stability of replication activity. PNS was pre-incubated at 4°C for 3, 24 and 48 h or PNS was diluted in dilution buffer (DB) or iodixanol and pre-incubated at 4°C for 24 h before a replication assay. Two last lanes show samples containing 1 mg/ml BSA or 100 μM 3'-dCTP. 18S rRNA was detected by in-gel hybridization from the same gel. (E) Stability of endogenous RNA. To detect endogenous SFV minus and plus strands, total RNA was isolated after the same pre-incubations as in D and analysed by in-gel hybridization with specific probes. (F) Detergent sensitivity. PNS samples containing the indicated detergent concentrations were incubated at 4°C for 1 h and either used for a replication assay or total RNA isolation followed by in-gel hybridization. After the replication assay, the incorporation of ^{32}P -CTP into 42S RNA was quantified and percentages indicate the incorporation compared to the untreated PNS. Lower panel shows the presence of endogenous minus strand RNA in the untreated and 1% detergent samples detected by in-gel hybridization. Numbers below the lanes indicate the percentage of ^{32}P -signal compared to the untreated sample.

Figure 2. Spherule location and replication activity. At 4 h p.i. PNS samples were prepared from SFV-infected (MOI 500) BHK cells, treated with 100 nM wortmannin at 1.5 h p.i. or 5 μM nocodazole at 0 h p.i. or untreated. These samples were compared to the PNS samples prepared from SFV-infected (MOI 50) untreated cells to give the percentages indicated in A-C. Error bars represent standard deviations for two independent experiments. (A and B) Total RNA was isolated from the PNS samples and plus- and minus-strand RNA were detected by in-gel hybridization with

815 specific probes followed by quantification of 42S RNA. (C) *In vitro* incorporation of ³²P-CTP into
816 viral RNA. 42S RNA was quantified.

817

818 **Figure 3. Schematic of RC isolation and purification.** Overview of the purification from cell
819 harvesting to iodixanol density-gradient centrifugations. From the sedimentation gradient, band 3
820 was collected for further purification by flotation. Band 2 obtained after the flotation represents
821 the purified RCs.

822

823 **Figure 4. Distribution of proteins, lipids and RNA in the S7 and P7 fractions.** PNS was prepared
824 from mock or SFV-infected (MOI 500) BHK cells treated with wortmannin and separated into an S7
825 supernatant and P7 pellet. (A and B) Protein and lipid profiles of PNS, S7 and P7 in an SDS-
826 polyacrylamide gel stained with Coomassie blue (A) or Sudan Black B (B), respectively. Numbers on
827 the left indicate the molecular masses (kDa) of marker proteins. (C) Distribution of viral and
828 cellular markers as studied by Western blotting. PMCA was used as a marker for the plasma
829 membrane, GM130 for the Golgi, calnexin for the endoplasmic reticulum, SDHA for the
830 mitochondria, Rab7 for the late endosomes, and β-actin for the cytosol. Numbers in parentheses
831 indicate the percentage of the protein present in the S7 fraction of that in PNS. The first number is
832 from mock samples and the second one from virus-infected samples. (D) Incorporation of ³²P-CTP
833 into SFV RNA in PNS, S7 and P7 prepared from SFV-infected cells. Numbers below the lanes
834 indicate the amount of incorporation into 42S RNA as a percentage of the label incorporated in
835 PNS. (E) Distribution of endogenous minus- and plus-strand RNA analysed by in-gel hybridization
836 from PNS, S7 and P7 prepared from SFV-infected cells. As a control, a probe against 18S rRNA was
837 used. Numbers below the lanes indicate the amount of 42S RNA as a percentage of that in PNS.

838

839 **Figure 5. Infection modulates cellular membranes.** S7 was prepared from mock- and SFV-infected
840 (MOI 500) BHK cells treated with wortmannin, and RCs were purified by a 3-h sedimentation in a
841 10-20% iodixanol step gradient. After centrifugation, gradients were fractionated (fr. 1-12, from
842 the top to the bottom; fr. 13, the pellet) and compared to S7. On the left, fractions from mock and
843 on the right from SFV sample. Protein (A) and lipid (B) patterns were studied in an SDS-
844 polyacrylamide gel stained with Coomassie blue or Sudan Black B, respectively. Numbers on the
845 left indicate the molecular masses (kDa) of marker proteins. (C) Western blotting shows the
846 distribution of viral and cellular markers as in Fig. 4. Furthermore, Na,K ATPase was used as an

847 additional marker for the plasma membrane, LAMP-2 for the late endosomes and lysosomes, and
848 CLIMP-63 and RTN4B as additional markers for the endoplasmic reticulum (sheets and tubules,
849 respectively). The sample volumes loaded from the fractions in the Coomassie or Sudan-stained
850 gels (A and B) and Western blot-gels (C) were about five and seven times larger, respectively, than
851 the sample volume loaded from the original S7 shown on the right.

852

853 **Figure 6. SFV RCs concentrate with the plasma membrane, ER and late endosome markers.** Light-
854 scattering band 3 from the sedimentation gradient was further purified by an 18-h flotation in a
855 10-30% iodixanol step gradient. After centrifugation, gradients were fractionated (fr. 1-12, from
856 the top to the bottom; fr. 13, the pellet) and compared to S7. On the left, fractions from mock and
857 on the right from SFV sample. Protein (A) and lipid (B) patterns were analysed in an SDS-
858 polyacrylamide gel stained with Coomassie blue or Sudan Black B, respectively. Numbers on the
859 left indicate the molecular masses (kDa) of marker proteins. (C) Distribution of viral and cellular
860 markers studied by Western blotting as in Fig. 4. (D) Distribution of Na,K ATPase (plasma
861 membrane), LAMP-2 (late endosomes and lysosomes), and CLIMP-63 and RTN4B (endoplasmic
862 reticulum sheets and tubules, respectively) between flotation fractions 3-5 was analysed and
863 compared to S7 by Western blotting. The sample volumes are as in Fig. 5.

864

865 **Figure 7. Purified RCs remain active in RNA synthesis.** (A) Distribution of endogenous minus- and
866 plus-strand RNAs between SFV sedimentation (left) and flotation (right) fractions studied by in-gel
867 hybridization. 18S rRNA was detected from the same fractions. Fr. 1-12, from the top to the
868 bottom. Fr. 13 is the pellet and S7 is shown for comparison. (B) *In vitro* replication activity of the
869 same fractions as in A studied by ³²P-CTP incorporation. (C) Comparison of *in vitro* replication
870 activity of S7 and purified RCs after replication reactions were incubated 4 h. S7 and RCs indicate
871 ³²P-CTP incorporation by the S7 fraction and the purified RCs, respectively. In A the volume from
872 the fractions used for RNA isolation was about ~7.5 times larger compared to the S7 sample
873 volume and in B and C 20-fold diluted S7 was used.

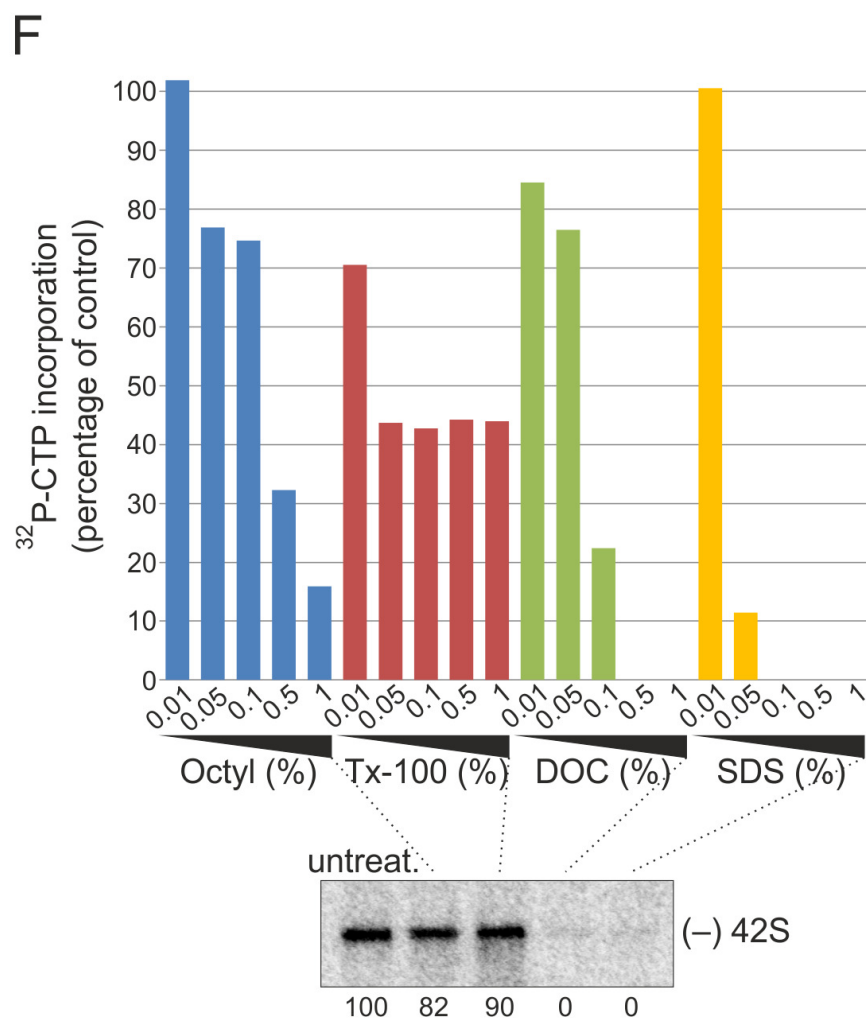
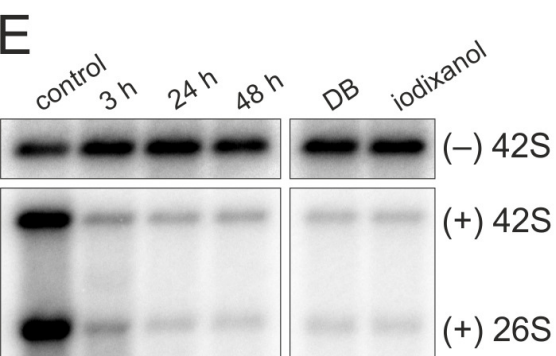
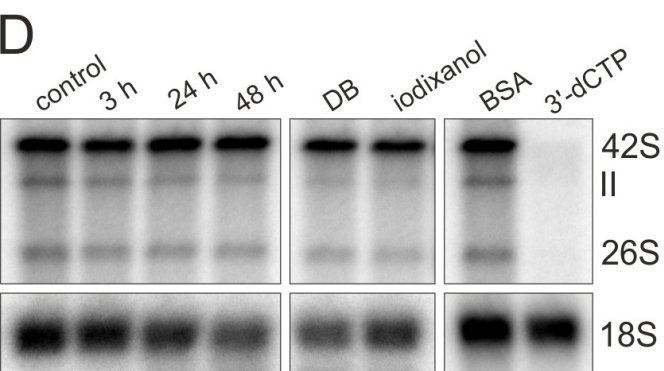
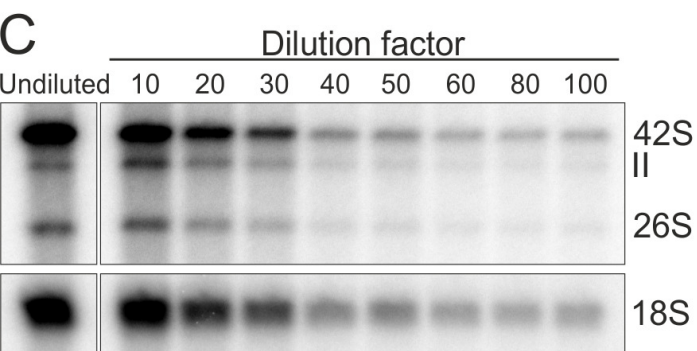
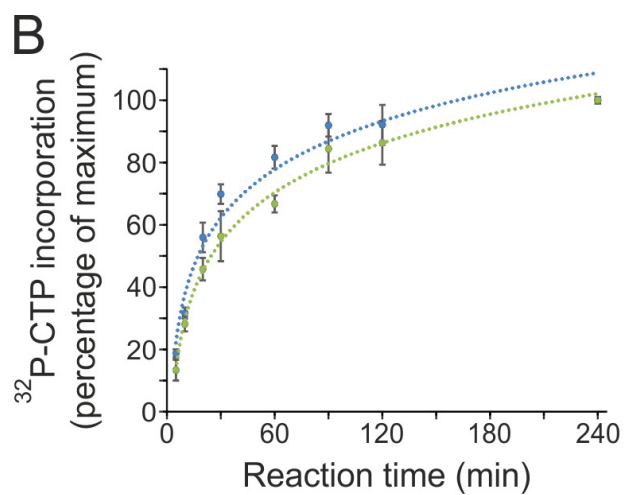
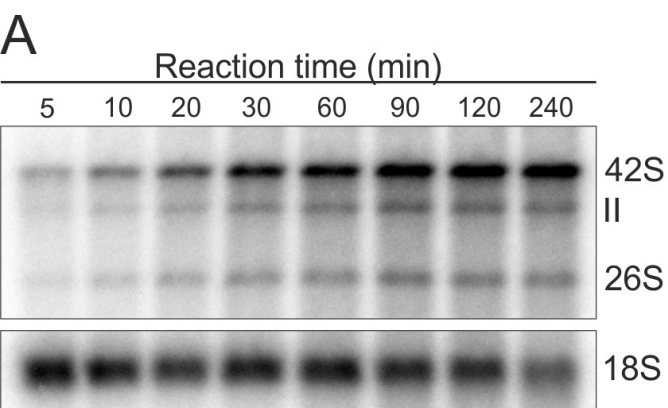
874

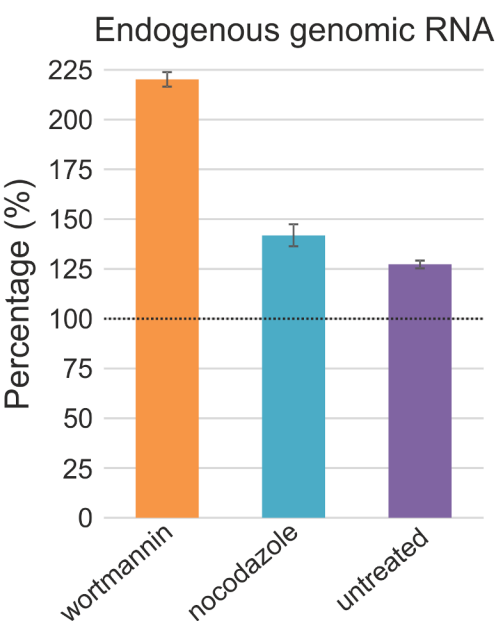
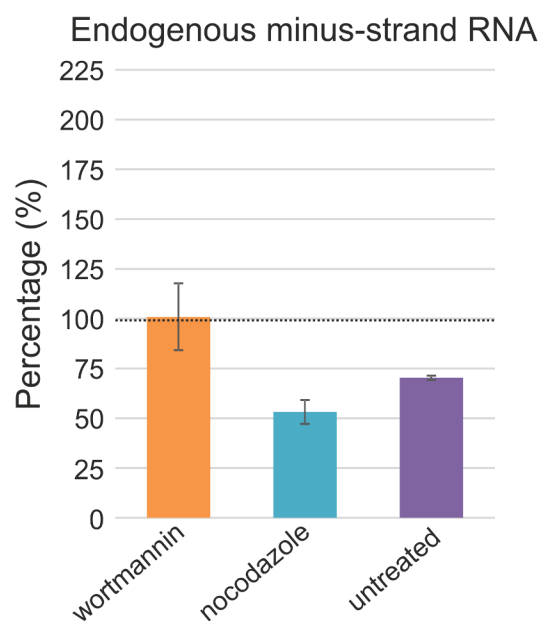
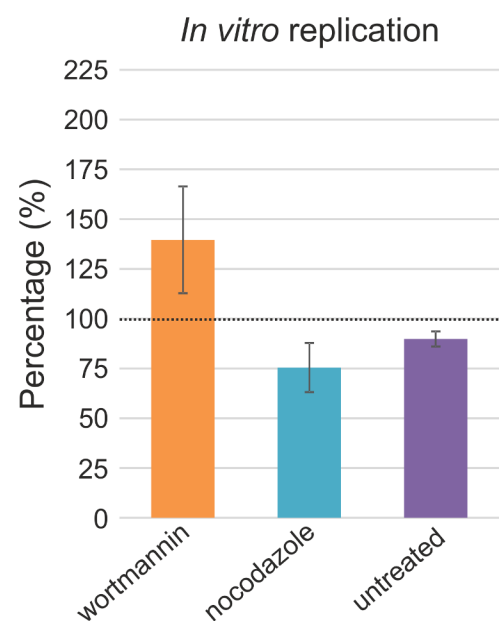
875 **Figure 8. Purified RC membranes contain spherule-like structures.** SFV RCs were purified in
876 subsequent sedimentation and flotation gradients, fixed and pelleted by differential centrifugation
877 for thin-section EM. Mock samples served as a control. All micrographs shown are from SFV
878 samples. (A) Membrane sheets observed in both SFV and mock sample. (B) Membranes with

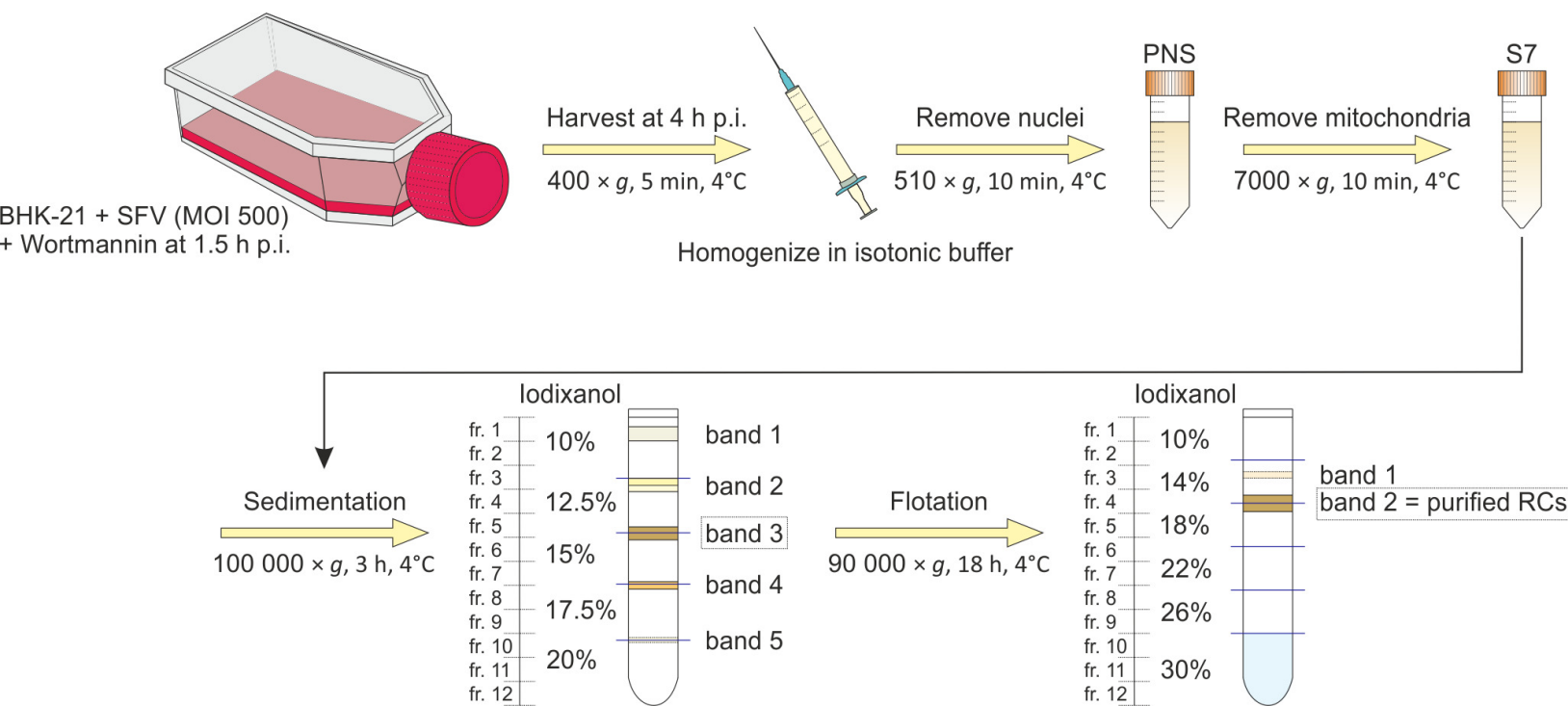
879 spherical invaginations of about 50 nm in diameter typical of SFV only. This represents most likely
880 plasma membrane sheets sectioned in a different orientation compared to A, resulting in vesicle-
881 like appearance. (C) Membrane sheet showing smaller round vesicles that may represent neck
882 parts of spherule-like structures, indicated by arrows. (D-I) Close-ups of spherule-like structures
883 indicated by arrows. In D white arrow heads indicate nucleocapsids. Scale bars, 1000 nm (A and B),
884 100 nm (C-F) or 50 nm (G-I).

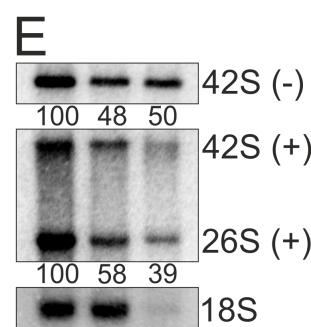
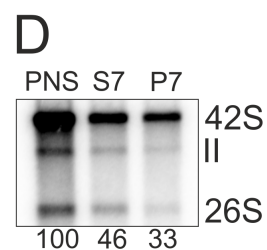
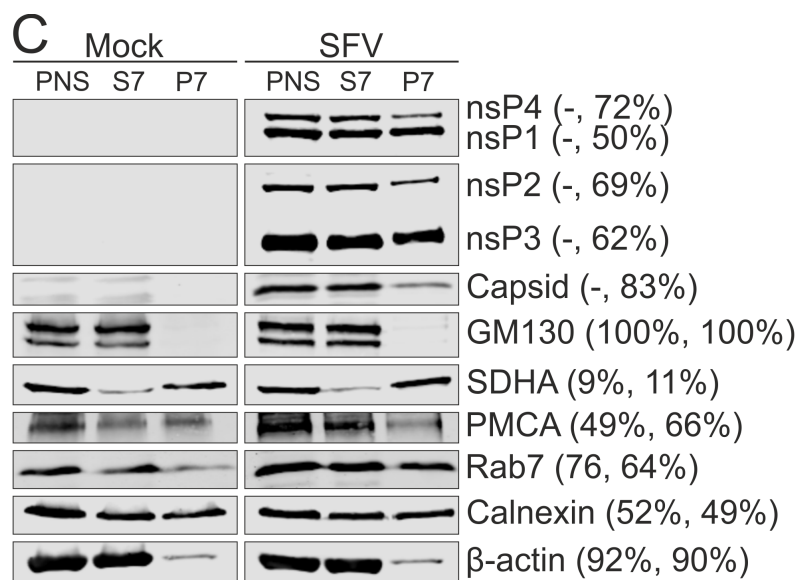
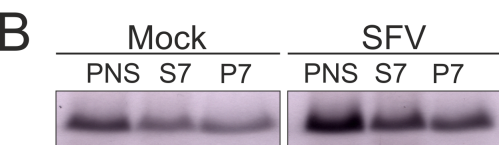
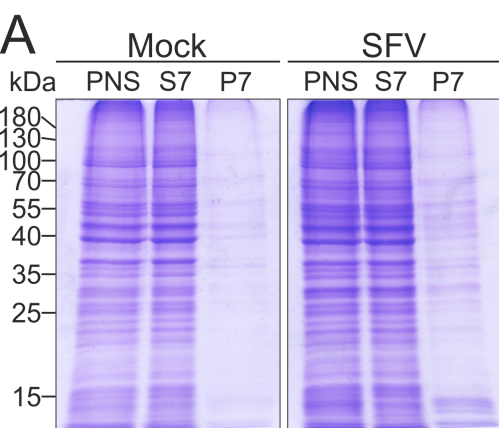
885
886 **Figure 9. Characterization of the *in vitro* replication activity of the purified RCs.** (A) Stability of
887 newly synthesized SFV genomic RNA. After a 60-min replication assay, ³²P-CTP incorporation was
888 blocked by the addition of 100 μM 3'-dCTP and incubation at 30°C was continued for an additional
889 180 min. Graph on the left represents an assay with 10-fold diluted S7 and on the right with the
890 purified RCs. At the indicated chase times radioactivity in 42S was quantified (yellow). As a control,
891 a reaction without 3'-dCTP was quantified (blue). In addition, *in vitro* transcript of Tmed added in
892 the reaction at a 0-min chase was quantified by in-gel hybridization (green). All values are
893 presented as percentages of the values at the 0-min chase. (B) Purified RCs and additional
894 exogenous template. Replication assay reactions were incubated 2 h. RCs indicates ³²P-CTP
895 incorporation by the purified RCs. RCs + Tmed RNA shows incorporation by the purified RCs after
896 an exogenous Tmed RNA transcript was added. As a control, ³²P-CTP incorporation by the P15
897 membrane fraction from cells transfected with the P1234 polyprotein and Tmed template
898 plasmids is shown and genomic and subgenomic (SG) Tmed are indicated. Lower panel shows the
899 presence of Tmed detected by in-gel hybridization. (C) Detergent stability and sensitivity. Purified
900 RCs were treated with 1% Tx-100 followed by an assay to detect replication (upper panel) and in-
901 gel hybridization to detect the minus-strand template RNA (lower panel). (D) ssRNA and RF/RI
902 forms of *in vitro* synthesized RNAs. After a 2-h replication assay with the purified RCs, RNA was
903 isolated and treated with RNase A/T1 or III under high salt conditions to specifically digest ssRNA
904 or dsRNA, respectively, and analysed in denaturing (left) or non-denaturing (right) conditions. (E)
905 Release of newly made RNA. A replication assay was performed with the concentrated purified
906 RCs and after 60, 120 and 180 min replication reactions, aliquots were removed to prepare pellet
907 and supernatant fractions followed by RNA isolation and analysis in a denaturing agarose gel. The
908 schematic shows how ³²P-CTP is incorporated into viral RNA during *in vitro* RNA synthesis resulting
909 in dsRNA containing both a plus strand synthesized in cells (indicated by magenta) and *in vitro*

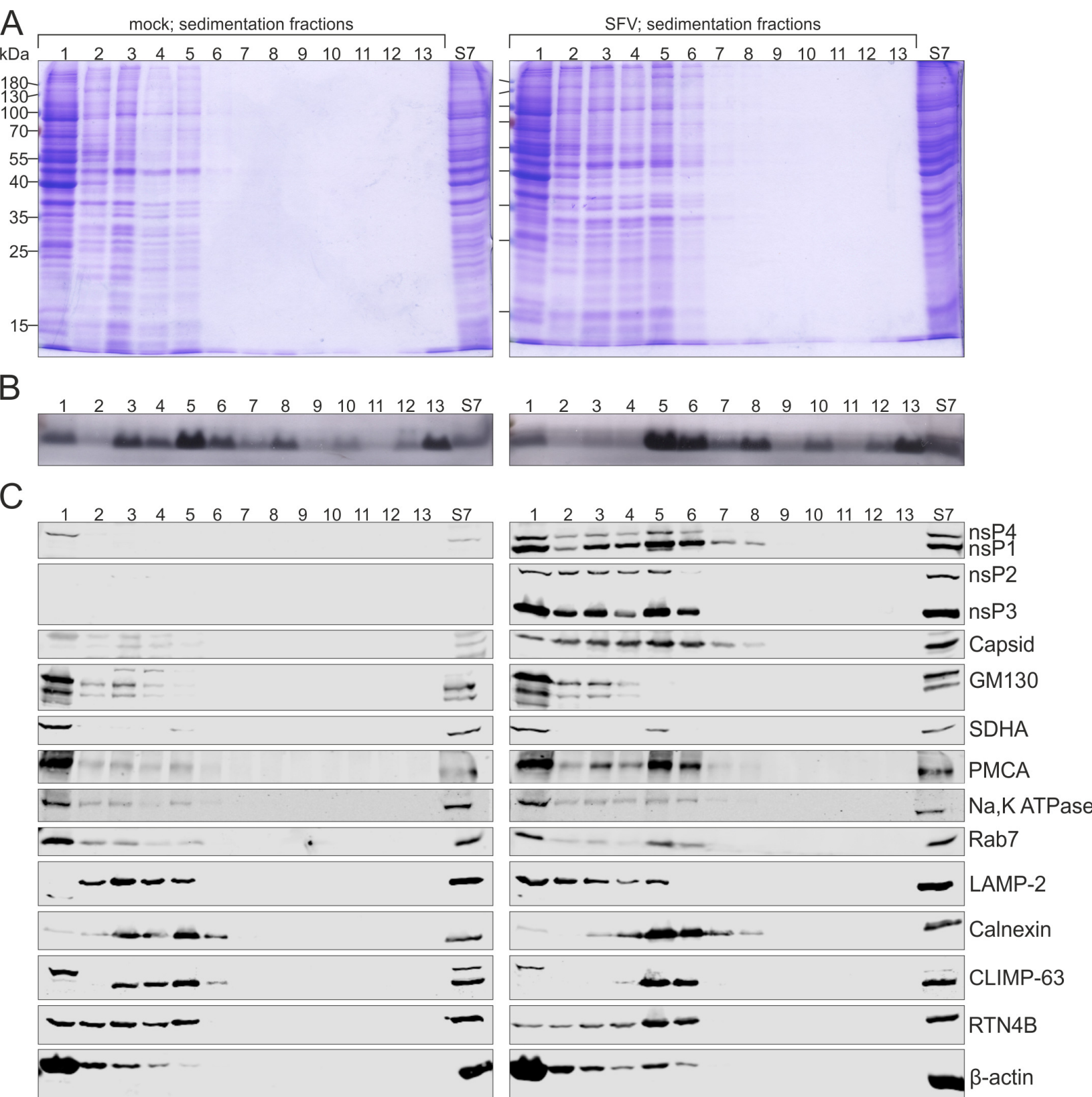
910 (indicated by orange). After a round of replication and release of the newly made plus strand, an
911 RC contains only the *in vitro* synthesized plus strand if replication is semi-conservative. (F) Increase
912 in the amount of RNA during *in vitro* replication. After a 4-h replication assay with the purified RCs
913 and unlabeled NTPs (indicated by NTPs), RNA was isolated and genomic RNA was detected by in-
914 gel hybridization. No NTPs indicates a reaction without added NTPs and ctrl indicates a sample
915 without any incubations before RNA isolation. 42S RNA was quantified and average percentages
916 from two independent experiments are shown in the table.

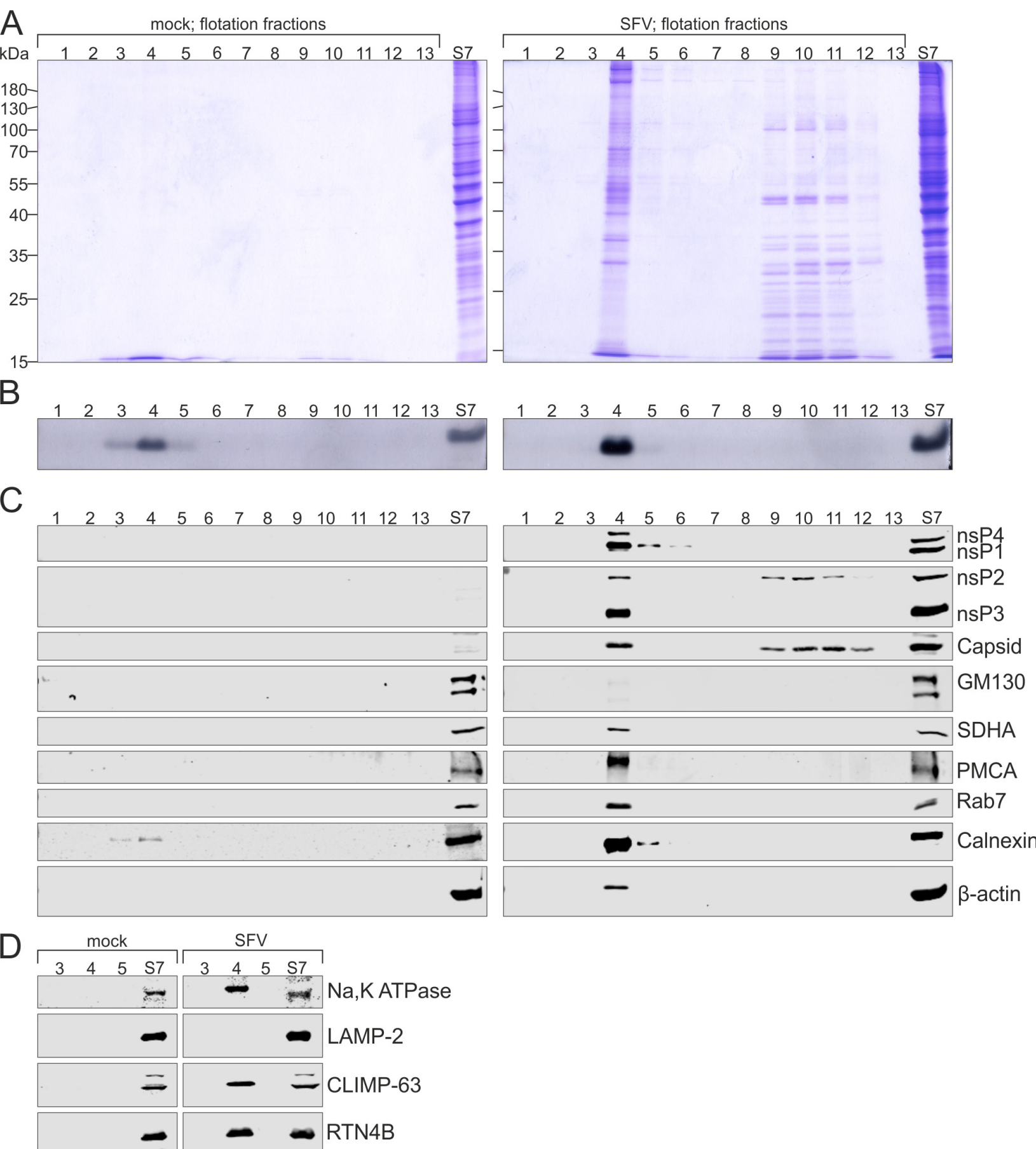


A**B****C**

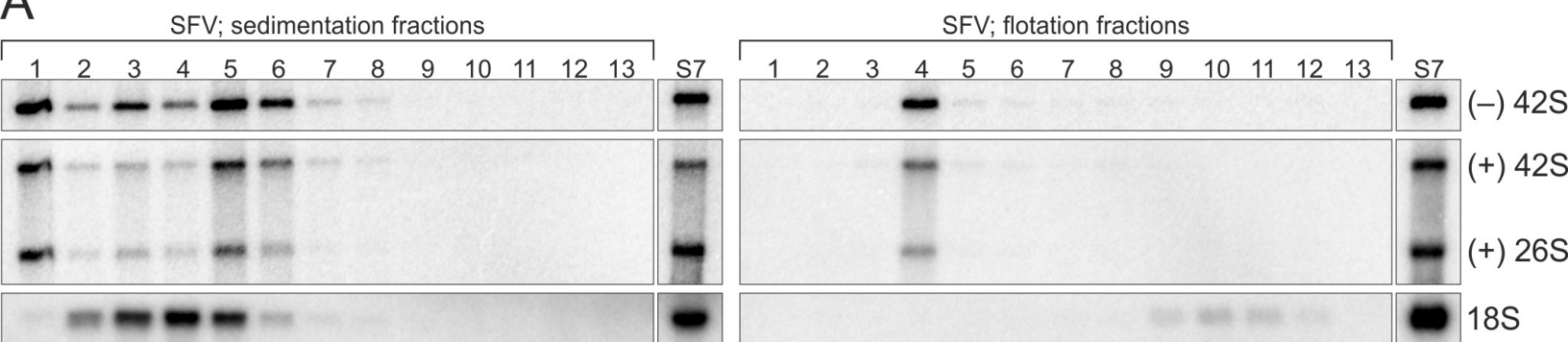




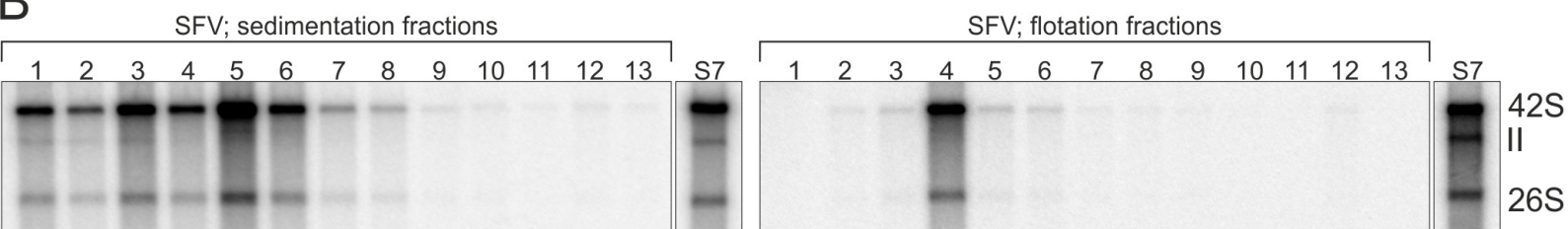




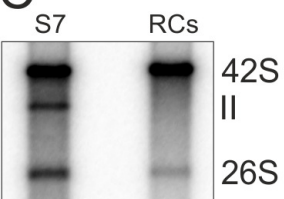
A

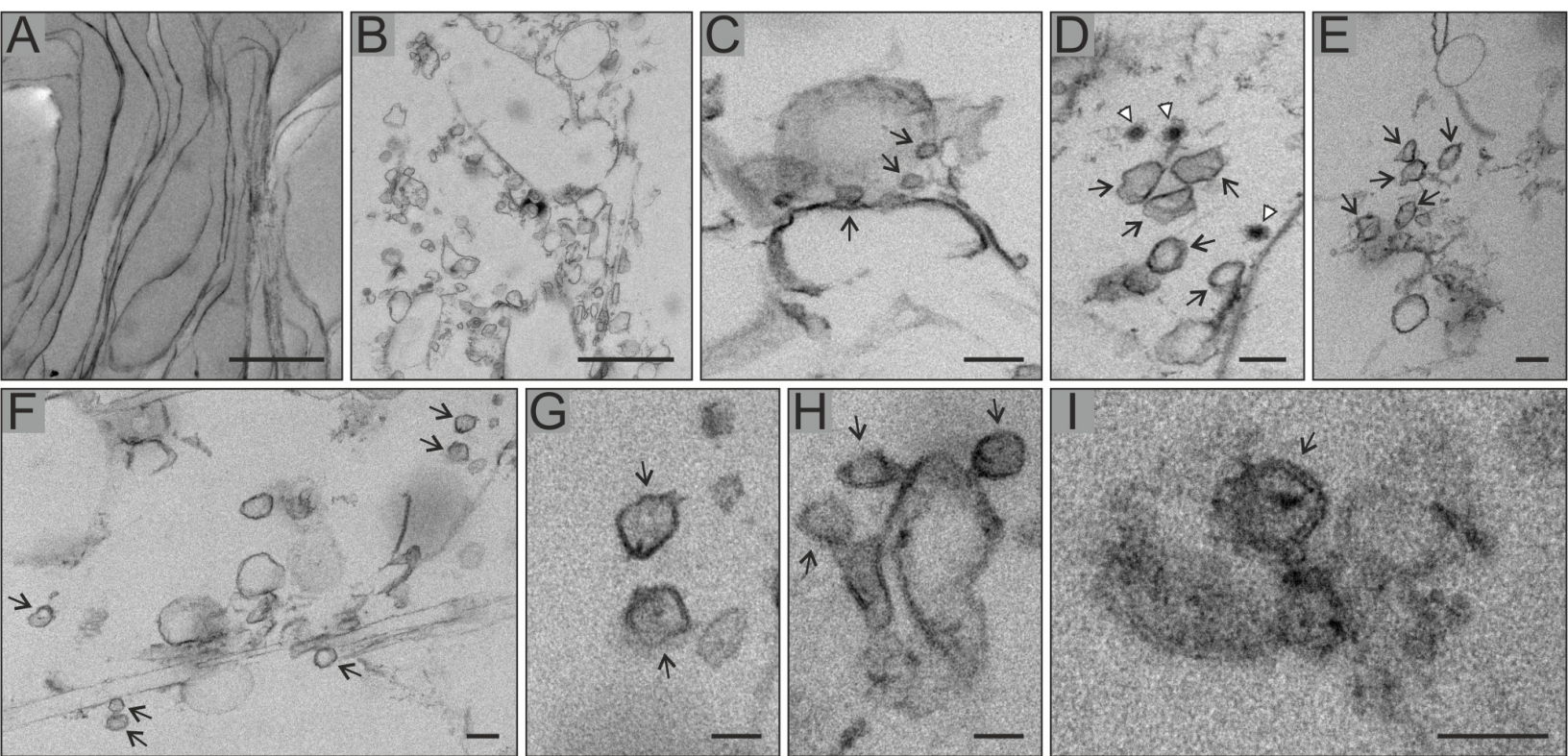


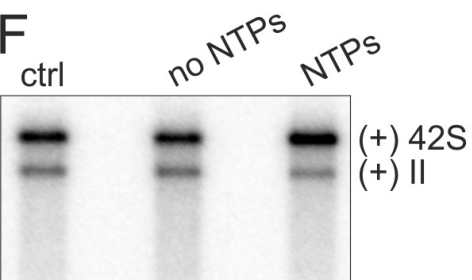
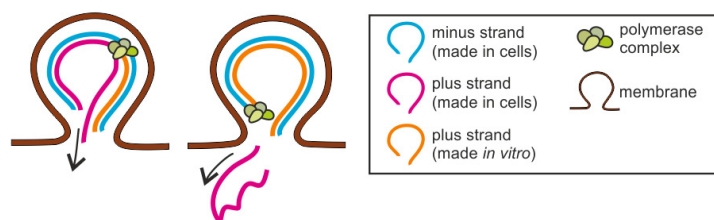
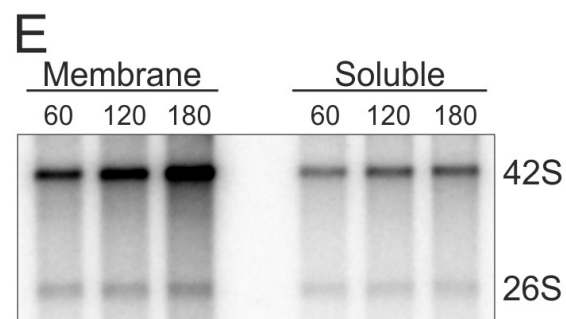
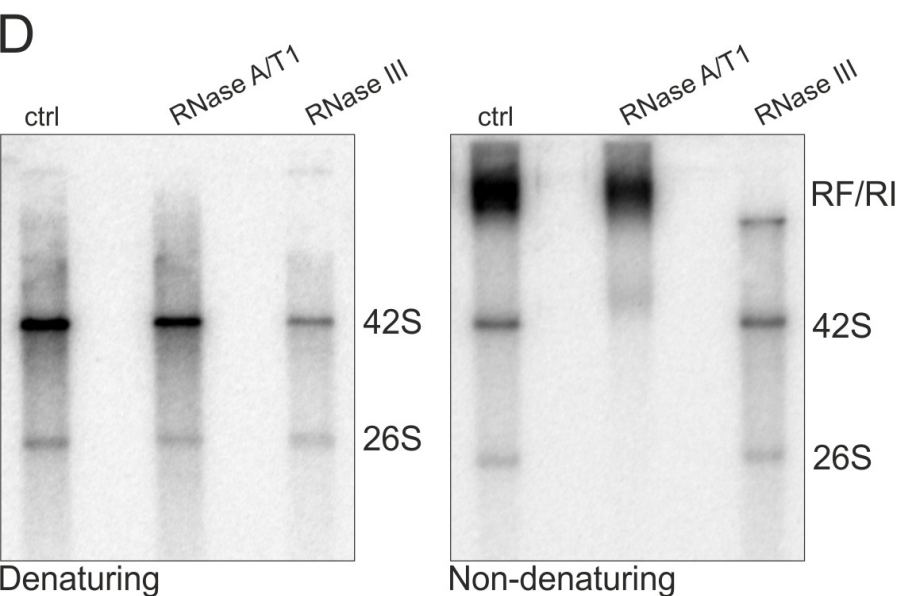
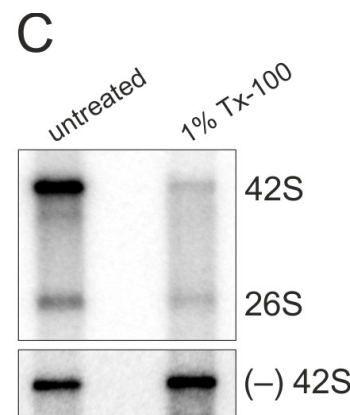
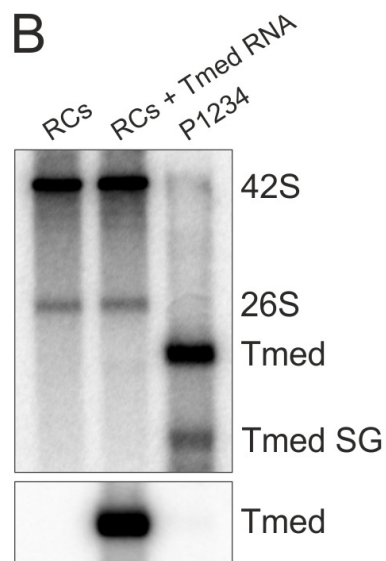
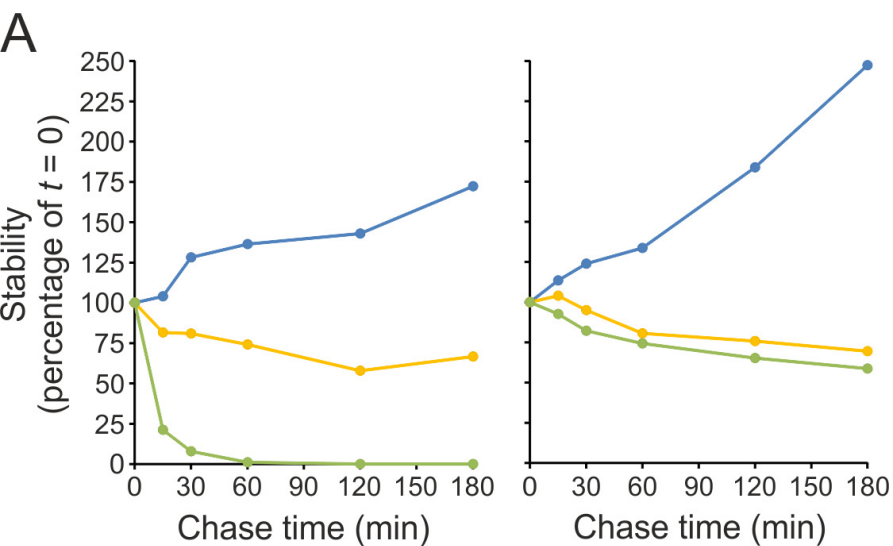
B



C







Binding of HybSFV4pos_8			
	NTPs vs. no NTPs	NTPs vs. control	Average
(+) 42S RNA	147	145	146